2016

Early modern human lithic technology from Jerimalai, East Timor

Ben Marwick
University of Wollongong, bmarwick@uow.edu.au

Christopher Clarkson
University of Queensland, c.clarkson@uq.edu.au

Sue O'Connor
Australian National University

Sophie Collins
Australian National University

Publication Details

Marwick, B., Clarkson, C., O'Connor, S. & Collins, S. (2016). Early modern human lithic technology from Jerimalai, East Timor. Journal of Human Evolution, 101 45-64.

Early modern human lithic technology from Jerimalai, East Timor

Abstract
Jerimalai is a rock shelter in East Timor with cultural remains dated to 42,000 years ago, making it one of the oldest known sites of modern human activity in island Southeast Asia. It has special global significance for its record of early pelagic fishing and ancient shell fish hooks. It is also of regional significance for its early occupation and comparatively large assemblage of Pleistocene stone artefacts. Three major findings arise from our study of the stone artefacts. First, there is little change in lithic technology over the 42,000 year sequence, with the most noticeable change being the addition of new artefact types and raw materials in the mid-Holocene. Second, the assemblage is dominated by small chert cores and implements rather than pebble tools and choppers, a pattern we argue pattern, we argue, that is common in island SE Asian sites as opposed to mainland SE Asian sites. Third, the Jerimalai assemblage bears a striking resemblance to the assemblage from Liang Bua, argued by the Liang Bua excavation team to be associated with Homo floresiensis. We argue that the near proximity of these two islands along the Indonesian island chain (c.100 km apart), the long antiquity of modern human occupation in the region (as documented at Jerimalai), and the strong resemblance of distinctive flake stone technologies seen at both sites, raises the intriguing possibility that both the Liang Bua and Jerimalai assemblages were created by modern humans.

Disciplines
Medicine and Health Sciences | Social and Behavioral Sciences

Publication Details
Marwick, B., Clarkson, C., O'Connor, S. & Collins, S. (2016). Early modern human lithic technology from Jerimalai, East Timor. Journal of Human Evolution, 101 45-64.

Early Modern Human Lithic Technology from Jerimalai, East Timor

Ben Marwick (1), Chris Clarkson (2) Sue O'Connor (3) and Sophie Collins (3)

1. Department of Anthropology, University of Washington, Box 353100, Seattle, WA 98195-3100 USA, & Centre for Archaeological Science, University of Wollongong, NSW, Australia.

2. School of Social Science, University of Queensland, W211, Seddon Building West (82E), The University of Queensland, St Lucia Qld 4072, Australia

3. Department of Archaeology and Natural History, The Australian National University, H.C. Coombs Building 9, The Australian National University, Canberra ACT 0200, Australia

Corresponding author:
Ben Marwick
telephone. (+1) 206.552.9450
fax. (+1) 206.543.3285
email. bmarwick@uw.edu

Abstract

Jerimalai is a rock shelter in East Timor with cultural remains dated to 42,000 years ago, making it one of the oldest known sites of modern human activity in island Southeast Asia. It has special global significance for its record of early pelagic fishing and ancient shell fish hooks. It is also of regional significance for its early occupation and comparatively large assemblage of Pleistocene stone artefacts. Three major findings arise from our study of the stone artefacts. First, there is little change in lithic technology over the 42,000 year sequence, with the most noticeable change being the addition of new artefact types and raw materials in the mid-Holocene. Second, the assemblage is dominated by small chert cores and implements rather than pebble tools and choppers, a pattern we argue is common in island SE Asian sites as opposed to mainland SE Asian sites. Third, the Jerimalai assemblage bears a striking resemblance to the assemblage from Liang Bua, argued by the Liang Bua excavation team to be associated with *Homo floresiensis*. We argue that the near proximity of these two islands along the Indonesian Island chain (c.100km apart), the long antiquity of modern human occupation in the region (as documented at Jerimalai), and the strong resemblance of distinctive flake stone technologies seen at both sites, raises the intriguing possibility that both the Liang Bua and Jerimalai assemblages were created by modern humans.

Key words: East Timor; Pleistocene; Stone artifacts; Reduction sequence; Modern human behaviour; *Homo floresiensis*

Introduction

Archaeological evidence of Pleistocene occupation of Sundaland and Wallacea plays a key role in understanding the origins and dispersal of modern humans because hominin movement into this area required solving novel problems such as travelling across open water between islands, exploiting unfamiliar environments and potentially interacting with other hominin species for the first time (Balme et al., 2009; Davidson, 2010; Morwood et al., 2005). Large stone artefact assemblages that span long time periods are rare in island SE Asia, thus limiting our ability to investigate these topics in detail. In this paper, we report on a large flaked stone assemblage from the Jerimalai rockshelter in East Timor, which spans the last 42,000 years.

Located on the edge of Wallacea, this location is significant because of its close proximity to northern Australia, representing one possible launching point for the long ocean voyage to Sahul. There are few well-reported assemblages from this region where people had accomplished early open water sea crossings and had well developed maritime technology. The long time span covered by this assemblage makes it potentially relevant to questions of historical change, environmental adaptation, and the relationship between modern humans and other hominin species in the region. While Jerimalai is only one location on the landscape, comparing its sequence to other well-documented sequences in the region may reveal insights into the process of human colonisation of island Southeast Asia (ISEA) and hominin replacements. Jerimalai is an ideal site to evaluate key issues in human evolution and the colonisation of island Southeast Asia and Sahul. This is because it has a rich record of lithic and organic artefacts that indicate early occupation of the region,

complex organic technology and marine exploitation that can be unequivocally linked to modern humans.

The aim of this paper is to describe the stone artefact assemblage from Jerimalai and evaluate its relevance to key issues in the early modern human colonisation of island Southeast Asia. In the following sections we describe the location of the site, the excavation methods and chronology of the archaeological deposit. After that, we briefly outline our Bayesian statistical methods, and then present the results of the stone artefact analysis. We present data on artefact discard rates and artefact taphonomy to explore changing site use through time. We review the metric and technological characteristics of cores and unretouched flakes to characterise the patterns of reduction in the assemblage, and identify the distinctive reduction sequences and retouched artefact types found at the site. We conclude with a discussion of the implications of our results for early technology in island Southeast Asia and compare the assemblage to that from Liang Bua on the nearby island of Flores. In particular, we explore the strong resemblance between the Jerimalai and Liang Bua assemblages that in our view calls into question the association between the Liang Bua artefacts and the *Homo floresiensis* hominin remains.

Site location and excavation

Jerimalai is a small limestone rockshelter located on the eastern tip of the island of East Timor (Figure 1). This is one of the closest points in ISEA to Australia and is often considered a likely staging point for the human colonisation of Australia (Birdsell, 1977). It is also at the edge of the Oriental and Australasian biogeographical

regions, marked by Weber's Line and Lydekker's Line. Weber's Line encloses the region in which the mammalian fauna is exclusively Australasian and Lydekker's Line marks the limit of Australian-New Guinean mainland fauna (Lohman et al., 2011). Although these lines are permeable, they highlight the striking faunal discontinuities observed in this region. Initial human movement across this region may have required adaptive and technological flexibility because of the need to adjust hunting and subsistence behaviours to incorporate new subsistence strategies as the humans colonised further south and east.

The rockshelter is located on an uplifted ancient Pleistocene reef, about 5 km from the current shoreline. Two squares of one square metre each were excavated in 2005 by Sue O'Connor to a depth of about 150 cm below the surface. The excavations and deposit have been previously described in extensive detail (including section drawings and site plans) by O'Connor (2007) and O'Connor et al. (2011) so here we report only new data about the chronology of the site and the stone artefact analysis. The site produced a rich assemblage of cultural material, including well-preserved faunal remains, a large number of stone artefacts (n = 9752), bone points, fishhooks, and shell beads dating to the terminal Pleistocene. We returned to the site in 2014 with the intention of enlarging the sample; however, further excavations were postponed indefinitely at the wishes of the local community.

Material and methods

Chronology of the excavated deposit

Table 1 summarises the results of 26 radiocarbon ages obtained from shells, and one from charcoal, from squares A and B (O'Connor et al., 2011; Reepmeyer et al., 2011). All radiocarbon dates were calibrated with the IntCal13 curve (Reimer et al., 2013) using the Bayesian algorithms in Bchron 4.1.2 (Parnell et al., 2011).

Human occupation at the site can be broken into four phases based on these dates (O'Connor et al., 2011). Square B contains the master chronological sequence due to the greater number of C14 ages, and analytical phases will be based on this chronology, while square A is fitted to this phasing. In square B, phase one spans 42-35 ka (spits 69-49) and corresponds to the lowest stratigraphic unit, while phase two spans the period 17-9 ka (spits 48-40). There is a stratigraphic break between these two phases and the Last Glacial Maximum (LGM) appears not to be represented in the chronostratigraphic sequence, either due to a lack of human occupation or erosion. Phase three (spits 39-21) spans the period 7 - 5.3 ka, and indicates a period of mid-Holocene occupation marked by relatively fast sedimentation rates and a change in marine fauna with a drop in the proportion of pelagic species relative to inshore species (O'Connor et al., 2011). O'Connor (2007) has previously noted that this period corresponds to the stabilisation of sea levels and establishment of a coastal environment near the site at the start of the Holocene. Finally, phase four (spits 20-3) is dated from 5.3 ka to recent times.

In square A, phase one corresponds to spits 46-39 and has an associated date of 42 ka from spit 39 (Table 1). Phase two is comprised of spits 38-26 with associated ages of between 17-10 ka. There is one inversion noted in spit 27 with a date of 22 ka. This

148 date potentially suggests that phase two contains material from eroded and deflated
149 LGM deposits, although the sequence from square B indicates that the volume of this
150 input is very low. Phase three consists of spits 25-6 and is associated with ages of 6.4-
151 5.5 ka, and phase four is covered by spits 5-1 with associated ages of 3-0 ka.
152 Combining corresponding phases from squares A and B allows the artefact
153 assemblages to be merged and analysed together rather than separately, generating a
154 greater sample size and more reliable results.
155
156 Based on rates of sediment deposition and the character of the sediment reported in
157 O'Connor et al. (2011), we identified substantial changes in the rate of deposit
158 accumulation at Jerimalai (Figure 2, Figure 3).
159
160 *Analytical methods*
161
162 The stone artefacts were identified according to the definitions in Table 2. For each
163 artefact we recorded a suite of basic metric measurements such as length, width,
164 thickness and mass. We also recorded a variety of technological attributes, including
165 the number and location of flake scars, cortex type and percentage, and platform type
166 and area. Where flakes showed signs of retouch, we recorded the retouch type and
167 length as well as measures of retouch intensity and curvature using protocols outlined
168 in Clarkson (2007). The data were analysed using R version 3.0.2 (R Core Team,
169 2015).
170
171 *Statistical methods*
172

We used two types of Bayesian methods, a one-way ANOVA for comparing groups of metric data (such as artefact measurements over different phases of occupation, where an ANOVA is the common null-hypothesis-significance-test, or NHST), and a Poisson exponential ANOVA for contingency table analysis (such as artefact counts, where a chi-square is the common NHST). For detailed discussion of methods, the motivation for using a Bayesian approach, see the SOM at http://dx.doi.org/10.6084/m9.figshare.985406.

The results of Bayesian tests are reported here as highest probability density intervals (HDIs) rather than more traditional *p* values (Krushcke, 2011), with more extensive output presented in the SOM . The HDI is the range of values that contain 95% of the values in the posterior distribution produced by the MCMC sampling. We identify a credible difference between sample measurements when the highest probability density interval does not include zero. This is analogous to a significant difference inferred from $p < 0.05$. Our SOM also includes the equivalent null-hypothesis-significance-test for direct comparison by readers who are unfamiliar with Bayesian tests.

Reproducibility and open source materials

To enable re-use of our materials and improve reproducibility and transparency (cf. Marwick, 2016), we include the entire R code used for all the analysis and visualizations contained in this paper in our SOM at http://dx.doi.org/10.6084/m9.figshare.985406. Also in this version-controlled compendium are the raw data for all the tests reported here, as well as an R package

that makes these methods, especially the Bayesian ANOVA and Bayesian chi-square, available for use with other datasets. All of the figures, tables and statistical test results presented here can be independently reproduced with the code and data in this repository. In our SOM our code is released under the MIT licence, our data as CC-0, and our figures as CC-BY, to enable maximum re-use.

Results

Raw materials

Table 3 shows the distribution of raw materials of complete flakes in each depositional phase at square B. Table 4 shows that the HDI distributions are close to zero, but only the change from phase four to five shows no credible differences in the interactions between raw material and phase. While this is a statistically significant result, it is not substantive because of the small changes in the low frequencies of quartz, quartzite and silcrete in the earlier phases, as shown in Table 3. Chert is uniformly dominant throughout the site, with silcrete, volcanic rock, quartzite and quartz present in much smaller quantities. Chert is available in stream beds within a kilometre of the site. A notable appearance in the Holocene deposits is six obsidian flakes (Figure 4), out of a total of ten obsidian pieces, some appearing in the Pleistocene. Compositional analysis of these obsidian pieces by Reepmeyer et al. (2011) showed that they did not match with a small sample from Indonesian and Philippine obsidian sources, but matched with artefacts from other archaeological sites in Timor. A local obsidian source has not yet been identified, but the Jerimalai obsidian comes from the same source as other sites on the island, Matja Kuru 1 and 2,

Bui Ceri Uato and Bui Ceri Uato Mane on the Baucau Plateau (Ambrose et al., 2009). Reepmeyer et al. (2011) suggest that these obsidian pieces were not obtained by direct access and instead come from a non-local source, hinting at participation in a wide-area exchange network.

The chert artefacts have a combination of rounded cortex (35%) and angular cortex (65%) suggesting that it probably comes from a combination of redeposited nodules recovered from creek beds and nodules and veins in the local limestone formations (cf. Environment and Development Division, 2003). For the remainder of the analysis we focus on the chert component of the assemblage since this makes up the greater part of the assemblage. By focussing only on chert we control for the influence of variation in the mechanical properties of different raw materials on patterns of artefact manufacture, use and discard.

Discard rates

Figure 3 shows the discard rate in chert complete flakes per cubic metre for each spit. From 30 ka to 20 ka there are low densities of artefacts and low sediment deposition rates. This represents decreased use of the site during glacial maximum conditions when the site was distant from the coast. Chert discard rates increase substantially in the mid-Holocene when sea levels stabilised at their current position. The mean discard rates per cubic metre per thousand years in each depositional phase similarly show the mid-Holocene peak in phase four and the low rates of discard during the LGM in phase two (Figure 3).

Artefact taphonomy

An important factor that needs to be considered when interpreting trends in artefact discard are taphonomic processes that may have increased the number of artefacts at one time relative to other times, independent of any major technological or depositional change (Bertran et al., 2012; Hiscock, 2002). By comparing the proportion of complete flakes, transversely and longitudinally broken flakes and flake fragments in each depositional phase we can identify differences in rates of flake fragmentation that may be indicative of variation in taphonomic or technological processes.

Table 5 shows that that there is a slight increase in the proportion of broken flakes to complete flakes in phases containing more artefacts. Table 6 shows that there are credible differences in the frequencies of breakage types over time, but that the size of the differences is small (i.e. the HDI 95% intervals are close to zero). The positive deflection of the HDI in Table 6 for phases three and four indicates that the frequency of broken artefacts is higher than expected during this time. This suggests that there have been substantial changes in post-depositional taphonomic processes operating on the assemblage in more recent times. One simple explanation is that during times of increased activity at the rockshelter the rate of flake breakage increased. In part, this might be due to an increase in flaking events that produced broken flakes, but we suspect it was more likely due to an increase in trampling resulting in post-depositional transverse or longitudinal-transverse breaks. This result reinforces the overall interpretation of the assemblage as demonstrating little substantial

technological change over time, but it does hint at some increases in the intensity of human use of the site in more recent times.

Between 8 and 15% of chert artefacts in each depositional phase show signs of having been heated, such as potlid scars or surface crazing. There are credible interactions between exposure to heat and all depositional phases (Table 7), which we interpret as overall insubstantial variation in heat exposure. Although the differences are statistically meaningful, the total rates of accidental artefact exposure to fire or deliberate heat treatment does not appear to have contributed substantially to variation in discard rates between phases.

Metric and technological characteristics of cores and unretouched flakes

Table 8 summarises the basic metric attributes of these flakes for each depositional phase. In general, flakes are small in size and squarish in shape and vary little between depositional phases. Flake mass is credibly higher in the transitions from phases two to three and three to four (Table 9, see the SOM for additional details); however the differences are in the order of tenths of grammes and probably not indicative of substantial behavioural changes. Table 10 shows equivalent dimensions for cores and Table 11 shows only a credible change in core mass from phase one to two. Cores have consistently blocky proportions over time with a decrease in mass during the middle Holocene, consistent with an increase in the extent of core reduction during a time of high artefact discard (Figure 5).

Summaries of flake platform characteristics give some insights into platform preparation and core use. Flakes with a single flake scar on the platform are consistently the most abundant throughout the assemblage. Next most abundant are focalised platforms (where the platform is largely or entirely comprised of a ring crack), which reflect careful placement of the point of impact to minimize the size of the platform relative to the rest of the flake (Clarkson and Hiscock, 2011; Shipton et al., 2013). Although the interaction of platform and flake size is complicated, very small platforms can reflect choices made by the knapper to maximize the production of flakes from small amounts of raw material or raw material nodules that are small in size (Davis and Shea, 1998; Dibble, 1997; Sahle et al., 2014). This appears to be the case at Jerimalai, as we also see a small median area and area range of focalised-platform flakes, relative to the other platform types (Figure 6). Platform characteristics in the assemblage at suggest an efficient strategy for flake removals.

Although there are a small proportion of cortical platforms in each depositional phase, this does not appear to have been a primary core reduction location. Figure 7 shows that the average percentage of cortex on cores at the site is very low. There are no credible changes in core or flake dorsal cortex over time (Table 12), suggesting that the extent to which cores were reduced at the site, or before they were introduced to the site, did not change much over time. The presence of some ‘cores’ made from flakes, with can be only 50% cortex at most, is a potential confounder that might exaggerate the aggregate cortex values downward. However, the absence of cores of any type with >50% cortex suggests a general pattern of very few nodules brought into the site at the start of their use-life, raising the possibility that non-local raw materials were often exploited here.

Further evidence for a simple late-phase on-site core reduction strategy comes from the dorsal surface attributes on flakes. Table 8 shows that most flakes had three or more negative flake scars and Table 10 shows that cores typically have 10-12 scars. There is negligible change in these variables over time and they are consistent with relatively high levels of core reduction. Another possible indicator of high reduction comes from the high proportions of overhang removal (53-59% across the four depositional phases). Experimental and archaeological research suggests that higher proportions of overhang removal tend to occur during more advanced stages of assemblage reductions, and may relate to the knappers adjusting the core platforms to prepare them for the more difficult blows required to detach flakes from smaller or more awkward cores (Clarkson, 2007; Macgregor, 2005; Marwick, 2008). Individually, these variables are not sufficient to interpret reduction behaviours, but taken together, the high number of flake scars and high frequency of overhang removal hint at consistently high levels of core reduction at this site. This is suggestive of a systematic, simple and extensive core reduction strategy, as opposed to an assemblage where cores are tested with one or two flake removals and then discarded. To extrapolate, people seemed to want to extract a lot of usable flakes from their cores.

Core technology

A range of core reduction strategies are evident in the Jerimalai assemblage, and these show remarkable conservatism over the span of occupation. The range of core types includes multiplatform, single platform, bidirectional, bipolar, radial and Levallois-

like cores. All cores in the assemblage are small, most likely indicating that the parent nodules are small. The few cores with extensive cortex found in the assemblage are quite small, less than 8 cm in maximum dimension.

Figure 8 is a box plot of core mass by type for complete cores (n = 42). Radial and Levallois-like cores are the largest on average, but the single largest core in the assemblage is a single platform core (82.94 g). Multiplatform cores vary greatly in mass, and are often amongst the largest cores in the assemblage. Bipolar cores are the smallest in the assemblage. Consistent with overall size, single platform cores retain the most cortex on average (20%), followed by radial cores (10%), multiplatform cores (6%) and faceted flake cores (4%). Levallois-like cores and bipolar cores exhibit the least cortex (<4%). Levallois-like cores exhibit almost twice the number of flake scars on average as other cores in the assemblage (mean = 27±9 scars versus 15±5 on average). Single platform cores have the least scars on average (10±3).

We also consider the use of large flakes to produce invasive flakes from faceted and unfaceted platforms located on the dorsal edge as a common form of flake production at the site, even though these artefacts are, strictly speaking, retouched flakes rather than cores. These flake cores are sometimes termed truncated faceted pieces (after Dibble and McPherron, 2006), and probably represent an approach to generating large fresh flakes from smaller available raw materials in the form of larger flakes (Figure 9). The hypothetical reduction sequence for these pieces is shown in Figure 10 and indicates that flaking typically begins by selecting a steep lateral margin or creating a steep faceted edge on the dorsal surface. This surface is then used as a platform to strike invasive flakes from the ventral surface. Flake removal from the ventral surface

makes use of the pronounced convexities around the bulb of percussion to guide the removal of flakes with sharp edges. Flakes produced early in the sequence tend to have large portions of the original ventral surface remaining on the dorsal surface, and sometimes a Kombewa flake with a ring crack on both the dorsal and ventral surfaces may result (Figure 11, Nos 6 and 12). Sixty-three percent of flakes with some ventral portion remaining on the dorsal surface have faceted platforms.

This approach to flake production employs similar principles to Levallois flaking, by first using the natural lateral and distal convexities on the ventral surface and later using the convexities created by intersecting flake scars to continue to produce flakes that become increasingly Levallois-like in appearance (Figure 12). As flaking onto the ventral extends around more of the lateral margin, the debitage surface and the flakes removed acquire increasingly radial flake scar orientations. Several flakes with remnant ventral surface on their dorsal face as well as multidirectional flake scars are found in the assemblage, indicative of these mid-stages in reduction (Figure 12, No. 5). Large flakes removed from these extensive and radially flaked ventral surfaces may appear indistinguishable from conventional Levallois flaking of a nucleus rather than a flake (Figure 11). Likewise, several small faceted radial cores found in the assemblage with large flake removals resemble small Levallois cores (Figure 13). Levallois flaking strategies have been claimed to minimize raw material waste while maximizing the total number of artefacts and amount of cutting edge produced (Brantingham and Kuhn, 2001). Levallois characteristics among the Jerimalai cores are consistent with results of the flake analysis that suggest strategies of efficient use of stone were important throughout the occupation of the site.

Retouched artefacts

Retouched artefacts range from 4-9% of the assemblage in each phase with a slight decrease in the proportion from phases two to three and three to four, but overall no substantial differences in frequency of retouched flakes or length of retouched edge over time (Table 13). Further insight into retouching behaviours comes from looking at the location of the retouch and the size of the retouched flakes. Figure 14 shows that the preferred locations for retouch is the left lateral margin and the distal end, but during the earliest period of occupation there were also a few flakes that were retouched all around the perimeter. Figure 15 shows flakes with retouch are consistently larger than flakes without retouch. This is a notable finding because it suggests that people employed a minimum of two strategies of flake production. One strategy was to produce large numbers of small unretouched flakes, perhaps as tools themselves or perhaps to modify the geometry of the cores to enable the second strategy, which is the production of larger flakes that were often retouched.

Retouched flakes are mostly lightly retouched, with retouch typically forming irregular side, end, notched or denticulated edges in roughly equal proportions and sometimes in combination, although rare artefacts exhibit extensive steep and invasive retouch (Figure 16, No.6). Measures of retouch intensity were taken on 17 complete scrapers from across the sequence (Table 14) using measures such as the Geometric Index of Unifacial reduction (GIUR), percentage perimeter retouched and the Index of Invasiveness (II). All measures confirm the low levels of retouch intensity observed in the assemblage (GIUR = 0.51 ± 0.21, percent of perimeter retouched = 29 ± 14 %, II = 0.16 ± 0.13).

Several artefacts show stout retouched projections resembling points, gravers or piercers (Figure 17). In fact, all but one of these artefacts do not show the heavily crushed rotational fracture patterns typical of drill bits, but may still have acted as piercers on softer materials. One such tip does show bidirectional crushing on the margins and tip (Figure 17, No. 5).

Several unusual retouched artefacts are found. Two are bifacially retouched tips that could be snapped tips from small bifacial points (Figure 16, Nos 9-10). The items are too fragmentary to determine whether this was the case or not. Another unusual artefact is a large hammerstone and anvil that was recovered from square B spit 46, with the hammerstone weighing 634 g and measuring 85 mm in length. It has flake removals at one end, hammer crushing at the other end, and anvil pitting on both surfaces. Burins and burin spalls are also found in low numbers throughout the sequence, as are small numbers of fortuitous microblades.

Technological types

To further explore variation in the assemblage we used a set of technological classes to show variations in distinctive forms of artefacts between the five phases. Table 2 defines the classes that we identified in the assemblage. Note that a truncated faceted flake is different from a Levallois-like flake as a Levallois-like flake shows fully centripetal flaking to create convexities, whereas a truncated faceted flake principally uses the curvature of the ventral surface to achieve the same thing. Technologically, they derive from the same process, but represent different modes of attack and stages

in the process (Levallois is more likely later in the sequence when flake scars cover most of the old ventral surface). We refer to cores as Levallois to indicate that they have prepared platforms (i.e. faceted) adjacent to an upper core surface that has clearly operated as the main removal surface, with multiple large scars that run across more than 50% of the core face, in many cases closer to 80%. The upper and lower surfaces therefore show clear hierarchy, with a lower domed platform preparation surface and an upper, flatter, removal surface. Furthermore, the lateral and distal convexities have been prepared and maintained in many cases, with evidence of débortant flakes and well developed radial flaking on cores and Levallois flakes. Although one or two cores are clearly discoidal in that they have domed surfaces on both hemispheres with flake scars terminating at a central apex, with no sign of faceting steep platforms, these are in the minority. Some of these Levallois-like cores could be end stages of a series of radial flake removals from the ventral surfaces of larger flakes, and the Levallois removals may be the final stages of this reduction process.

Table 15 shows the distribution of these classes across the five depositional phases. Although there are subtle shifts in the distribution of artefact classes through time, the data in Table 15 are not suggestive of major changes in artefact technology over time. Our data support O'Connor et al.'s (2011) description of the phase one assemblage as dominated by faceted radial cores and side and end scrapers. In the Holocene phases, we observe a shift in the composition of the formal component of the assemblage to having more distal and lateral retouched flakes and multiplatform cores. The high number of spits containing flakes with facetted platforms, faceted flakes struck from the ventral surfaces of larger flakes, and redirecting flakes indicates the consistently

frequent reworking and maintenance of cores to extend their productivity. The presence of flakes and cores with Levallois-like features, most likely representing heavily reduced truncated faceted 'flake cores', further suggests a systematic use of faceting and radial flake removals during core reduction as described above. Spits 20, 23 and 24 contain striated haematite pieces (Figure 4), indicating possible artistic activity at around 5.8-6.0 ka. Rock art is found in nearby caves and it is therefore not surprising to find striated ochre pieces at the site.

Discussion

The assemblage from Jerimalai is a large but relatively simple assemblage that changes little over time. The main changes noted are a slight decrease in the frequency of Levallois-like flakes and cores after phase one, and an increase in the frequency of bipolar in phase two (terminal Pleistocene). The proportion of truncated faceted flakes with ventral remnants on the dorsal face (i.e. artefacts relating to 'flake cores') and the proportion of retouched flakes fluctuates over the phases and shows no obvious pattern of increase or decrease through time. A small increase in raw material diversity also occurs in the final phase (5.3 ka), with quartz and obsidian appearing in the final two phases. Also at this time there is a slight increase in flake size, but no major changes in core size in the final phase. Additional Holocene changes include the appearance of flakes with edge gloss in the middle Holocene in spits 4, 5, 20 and 27 in square B (5.5 - 6.6 ka, Figure 4), perhaps associated with new kinds of plant exploitation (most likely bamboo), and the first sign of earthenware pottery appearing after 5 ka.

Perhaps the most striking change is the discard rate, which is highest during the early Holocene in phase three (7 - 5.3 ka), and lowest during the terminal Pleistocene in phase two (17-9 ka). There are also increases in artefact breakage and heat altered artefacts from phase one to two, and two to three. This probably reflects an increase in human activity at the site, resulting in an increase in artefact use and discard, trampling of the surface and fires lit at the site. Previous attempts to identify variation in the use of artefacts at Jerimalai using microscopic analysis met with limited success due to poor preservation of micro-traces and obscuration of use-wear by adhering carbonate deposits (Hayes et al., 2014).

Levallois-like flaking strategies have been noted in ISEA before by Glover (1981) at Leang Burung 2 (Sulawesi), where Levallois point-like artefacts are said to occur. We emphasize the fact that although many features of the artefacts at Jerimalai resemble Levallois technique, they appear to result from the intensive exploitation of small flake cores by faceting (i.e. truncating) the perimeter and exploiting the natural convexities presented by the curvature of the ventral surface to produce flakes that are proportionally large relative to the surface of the core. However, one small pointed flake with a faceted platform that in some respects resembles a Levallois point was found in phase one, although we consider this likely to be fortuitous. True discoidal core reduction is also present only in the earliest two phases at the site.

The increase in the frequency of bipolar reduction at Jerimalai in the terminal Pleistocene may relate to increased aridity and risk at the tail end of the LGM, when mobility and uncertainty over resource access may have been greater. The apparent absence of occupation at the site during the LGM may be telling in itself, and appears

to mirror a trend across East Timor for site abandonment at this time. Interestingly, the nearby large cave of Lene Hara was occupied during the LGM, and the flake assemblage from this period will provide a valuable comparison and adjunct to that from Jerimalai. We might expect there to be an even greater use of bipolar reduction at Lene Hara at this time when aridity was at its greatest and when parts of the East Timorese landscape appear to have been unsuitable for longer-term habitation.

Overall, the stone artefact technology at Jerimalai suggests a highly stable system with only subtle changes over long time periods. The dominant flaking strategies of bipolar, truncated faceted flake core reduction and multiplatform core reduction are present throughout the entire 42 ka years of occupation at the site, with only small variations in frequency through time. In this respect, Jerimalai shares many technological characteristics with other Late Pleistocene sequences throughout island Southeast Asia.

Several sites in the Philippines have relevant Late Pleistocene assemblages suitable for comparison, such as Tabon Cave, Pilanduk Cave, Callao Cave, Ille Cave and Musang Cave (Détroit et al., 2004; Lewis et al., 2008; Mijares et al., 2010; Patole-Edoumba, 2009). Patole-Edoumba (2012) and Pawlik (2012) characterise these assemblages as showing only subtle variation across the islands, but with substantially similar sets of technological characteristics, and without showing major changes in manufacturing systems over the Pleistocene. The key changes in these sites, as at Jerimalai, are in choices of raw materials, which appear to be constrained by the unique details of the local availability of stone at each site (Mijares, 2014). Sample size is prohibitively small for Niah Cave in Borneo; however Barker et al. (2007)

observe that the assemblage is consistent with mobile foragers using nonselective hunting technologies. On Sulawesi, Glover (1981) noted continuity in stone artefact technology at Leang Burung 2 over the last 30,000 years.

Comparison with Liang Bua

There may be a temptation to describe these assemblages of simple and stable stone artefact technologies as a 'least effort approach' to stone tool manufacture. This label has been used for disparate assemblages as far back as the Olduwan (Reti, 2016). Our view is that although we agree that these simple technologies of ISEA share some basic 'least effort' attributes (such as the absence of visually distinctive and extensively retouched pieces) with other similarly-labelled assemblages worldwide, there are details in the Jerimalai assemblage that are distinct to ISEA and require further comparison and discussion. To date, the only site with a comparably large stone artefact assemblage that has been described in detail is Liang Bua on the nearby island of Flores.

The overall pattern of stone artefact technology at Liang Bua is one of continuity with only minor changes to the assemblage over the period of occupation (Moore et al., 2009). At Jerimalai and Liang Bua we find a number of distinctive forms of artefact: truncated faceted pieces (described as cores-made-on-flakes in the Liang Bua assemblage), ventral remnants of flakes struck from ventral surfaces of larger flakes (Figure 11, i.e. detachment scars at Liang Bua), Kombewa flakes (i.e. contact removal flakes at Liang Bua), burins and redirecting flakes, discoidal and multiplatform cores (Brumm et al., 2006; Brumm et al., 2009; Brumm et al., 2010; Moore and Brumm,

2007; Moore et al., 2009). The presence of the somewhat unusual 'flake truncations' found at Liang Bua are also present at Jerimalai in phases one to three.

Perhaps the most striking technological similarity linking these two sites is the presence of pieces with retouched projections. Those at Jerimalai (Figure 17) may be typologically equivalent to the chert 'perforators' at Liang Bua (Brumm et al., 2006; Brumm et al., 2010). These perforators have been argued to be present at Mata Menge, but our view is that the long narrow and extensively shaped projections of Liang Bua specimens are not equivalent to the three Mata Menge specimens illustrated in Brumm et al. (2006), which appear fortuitous rather than intentionally shaped like the Liang Bua specimens. These similarities between Jerimalai and Liang Bua are not due to the 'least effort approach' because they are not found in other well-described assemblages from ISEA, such as Mata Menge and Tabon Cave (Patole-Edoumba, 2009; Patole-Edoumba et al., 2012).

Further technological similarities between the Liang Bua and Jerimalai lithic assemblages can be identified. Moore et al. (2009) identify a group of larger flakes in their assemblage that appear to have been produced off-site and transported to the site where they are discarded as retouched flakes. A similar pattern is noted at Jerimalai where larger than average retouched flakes are transported to and discarded at the site in phases three and four. Core reduction also appears similar, with unit four, the main artefact bearing unit at Liang Bua, having an average number of core scars of 9.2 (Moore et al., 2009), while the range of averages at Jerimalai is 9-14.

595 Moore et al. (2009) have noted that the assemblages produced by *H. sapiens* and *H.*
596 *floresiensis* at Liang Bua are substantially the same. We find that Jerimalai also shares
597 similarities in the exploitation, use and discard of stone resources with Liang Bua. We
598 see this as perhaps the most significant implication of the Jerimalai assemblage. It
599 raises the question of whether the Liang Bua stone artefact assemblage was made in
600 fact uniquely by *H. floresiensis*, as suggested by Brown et al. (2004) and Moore and
601 Brumm (2009), or by modern humans behaving in much the same way as at Jerimalai,
602 or even by *H. floresiensis* who learned the techniques from co-existent *H. sapiens*.
603 We question links between the Liang Bua and Mata Menge stone artefact
604 assemblages because when we compare the frequency of artefact types at the two sites
605 we find a significant difference (χ = 843.48, df = 14, p = 0, HDI: 0.049-0.857). The
606 key differences are a higher proportion of discoidal and unifacial disc cores, and no
607 bipolar artefacts at Mata Menge, compared to Liang Bua. These differences may
608 simply reflect change over time, or different cultural traditions resulting from
609 different groups occupying the island. However, the differences also invite the
610 possibility that different hominid taxa created the assemblages at these two sites.
611
612 Reinterpretation of the Liang Bua stratigraphy and chronology by Sutikna et al. (2016)
613 dates the *H. floresiensis* skeletal remains to 100–60 ka and the associated stone
614 artefacts to 190-50 ka. This places the Liang Bua stone artefacts in a time period
615 when modern humans were present in the region, from Laos (Demeter et al., 2015),
616 possibly the Philippines (Mijares, 2010 and Detroit et al., 2013 claim it as a small-
617 bodied *H. sapiens*, but see Kaifu et al., 2015 for a dissenting view), to Australia
618 (Clarkson et al., 2015), so modern human involvement with the artefacts from Liang
619 Bua is plausible. However, currently available data from Liang Bua do not include

620 enough information to determine if most of the artefacts are closer to 50 ka or 190 ka
621 in age, based on the ages provided by Sutikna et al. (2016). With the revised dates,
622 additional information about the Liang Bua stone artefacts are necessary to
623 understand their ages. We welcome the Liang Bua researchers making publicly
624 available their raw data on artefact technology and provenance at Liang Bua, as we
625 have done for this study. Following Marwick (2016), the R code, raw data and SOM
626 supporting the text of this paper are freely available on the web at
627 http://dx.doi.org/10.6084/m9.figshare.985406
628
629 A final observation is that the rarity of choppers and large pebble artefacts in the
630 assembalge at Jerimalai is similar to many other sites in ISEA, such as Liang Bua,
631 Niah, Tabon, Ille and Callao Cave. This supports Moore and Brumm's (2007) claim
632 that previous notions of a regional pattern of Pleistocene assemblages of
633 'chopper/chopping-tool industries' and 'pebble-and-flake technocomplexes' in
634 Southeast Asia are inaccurate and should be discarded. Similarly, the dominance of
635 chert in this assemblage supports previous claims (Eren et al., 2011; 2014; Rabett,
636 2011; Reynolds, 1993) that the lack of fine-grained stone is not a compelling cause
637 for technological simplicity, for example, of the Southeast Asian record, contrary to
638 Mellars (2006) and Klein (2009).
639
640 **Conclusion**
641
642 Jerimalai shows few major changes over a long period of time. The key changes are
643 in discard rates and choice of raw materials. Discard rates are very low just prior to
644 the onset of the LGM and increase in the middle Holocene, when raw materials

become more diverse. The technological strategies of bipolar, truncated faceted flake core reduction and multiplatform core reduction are stable throughout the entire squence. These data from Jerimalai support the picture suggested by many other sites in the region of a stable technological system with only subtle changes during the Late Pleistocene and Holocene.

This pattern of relatively simple stone artefact technologies in ISEA appears to be at odds with indications of more complex technologies, such as fish hooks from Jerimalai (O'Connor et al., 2011), hafted projectiles (e.g. the bone artefact from Matja Kuru 2, also on the island of Timor, O'Connor et al., 2014a), and shell appliques and beads (from Jerimalai, Lene Hara, and Matja Kuru 1 and 2, Langley and O'Connor, 2015; 2016). On one hand, the stone artefacts and shells both show continuity over long periods at Jerimalai (Langley and O'Connor, 2016). On the other hand, we might ask why the stone artefacts were not modified in elaborate ways like the shell fish hooks and hafted bone projectile points? We favour the explanation of O'Connor et al. (2014a) that complex technologies were more often made from bone, shell or wood, rather than stone, perhaps because organic raw materials were easily accessible, they are similar to stone in many performance characteristics, and may have social/symbolic signficance. Stone was not completely neglected - microscopic analysis of a sample of stone artefacts from Jerimalai found use-wear traces on flake platforms, indicating that the flakes were once attached to a tool edge, suggesting composite tool construction (Hayes et al., 2014). The rarity of ancient complex organic artefacts in ISEA relative to Europe and Africa may be because these artefacts decay quickly in tropical climates, and because of the smaller number of sites and volumes of sediments studies in this region (Langley et al., 2011). Our view is that the

Pleistocene hafting and point manufacturing traditions in ISEA were largely confined to perishable raw materials, as products of either local independent invention (cf. South Asian Pleistocene microliths, Clarkson et al., 2009; Petraglia et al., 2009) or as part of the toolkit of the first modern human colonisers to arrive in the region With the previously described innovations in this region in fishing technology and organic artefacts (Langley et al., 2016; O'Connor et al., 2014b; 2011), local innovations in stone artefact technology seem like a highly plausible scenario.

While the simplicity of the Jerimalai assemblage may be in part due to a 'least effort approach' that is found in other assemblages in the region, such as Mata Menge, and may be traced back to the Olduwan, we have also identified a suite of distinctive technological features shared by other assemblages in ISEA. The most signficant finding of our anlaysis is that Jerimalai shares similarities in the exploitation, use and discard of stone resources with Liang Bua. The similarities are at odds with patterns identified elsewhere in the world that find increasingly derived technological elements that appear to be associated with the appearance of new *Homo* species through time (Foley and Lahr, 2003) In our opinion, this raises the intriguing possilibity that the assemblages at Jerimalai and Liang Bua were both made by, or under the influence of, *H. sapiens.*

Acknowledgements

SOC acknowledges the assistance and hospitality of the many East Timorese people who allowed access to the site, and actively participated in the excavtion and post-excavation fieldwork. Permissions for the archaeological excavation was obtained

from the Ministry of Art and Culture, East Timor. We would particularly like to thank Mrs Cecília Assis for facilitating this process. We would also like to acknowledge the support of the people of Tutuala who assisted with the excavation and without whom this research would not have been possible. The fieldwork in East Timor was funded by Discovery Grant DP0556210 to SOC from the Australian Research Council. BM was supported by Deutscher Akademischer Austauschdienst Fellowship A/14/01370-Ref.316, a UW-UQ Trans-Pacific Fellowship and an Australian Research Council Future Fellowship (FT140100101). CC was supported by an Australian Research Council Queen Elizabeth II Fellowship (DP110102864).

References cited

Ambrose, W., Allen, C., O'Connor, S., Spriggs, M., Oliveira, N.V., Reepmeyer, C., 2009. Possible obsidian sources for artifacts from Timor: Narrowing the options using chemical data. J Archaeol Sci 36, 607-615.

Balme, J., Davidson, I., McDonald, J., Stern, N., Veth, P., 2009. Symbolic behaviour and the peopling of the southern arc route to Australia. Quaternary International 202, 59-68.

Barker, G., Barton, H., Bird, M., Daly, P., Datan, I., Dykes, A., Farr, L., Gilbertson, D., Harrisson, B., Hunt, C., 2007. The 'human revolution' in lowland tropical Southeast Asia: the antiquity and behavior of anatomically modern humans at Niah Cave (Sarawak, Borneo). J Hum Evol 52, 243-261.

Bertran, P., Lenoble, A., Todisco, D., Desrosiers, P.M., Sørensen, M., 2012. Particle size distribution of lithic assemblages and taphonomy of Palaeolithic sites. J Archaeol Sci 39, 3148-3166.

Birdsell, J.B., 1977. The recalibration of a paradigm for the first peopling of Greater Australia. Sunda and Sahul: Prehistoric Studies in Southeast Asia, Melanesia and Australia, 113–167.

Brantingham, P.J., Kuhn, S.L., 2001. Constraints on Levallois core technology: A mathematical model. J Archaeol Sci 28, 747-761.

Brown, P., Sutikna, T., Morwood, M.J., Soejono, R.P., et al., 2004. A new small-bodied hominin from the Late Pleistocene of Flores, Indonesia. Nature 431, 1055.

Brumm, A., Aziz, F., van den Bergh, G.D., Morwood, M.J., Moore, M.W., Kurniawan, I., Hobbs, D.R., Fullagar, R., 2006. Early stone technology on Flores and its implications for Homo floresiensis. Nature 441, 624-628.

Brumm, A., Kurniawan, I., Moore, M.W., Suyono, S., R., Jatmiko, Morwood, M.J., Aziz, F., 2009. Early Pleistocene stone technology at Mata Menge, central Flores, Indonesia, in: Aziz, F., Morwood, M.J., van den Bergh, G.D. (Eds.), Pleistocene Geology, Palaeontology and Archaeology of the Soa Basin, Central Flores, Indonesia. Geological Survey Institute Bandung. Special Publication, Bandung, pp. 119–137.

Brumm, A., Moore, M.W., van den Bergh, G.D., Kurniawan, I., Morwood, M.J., Aziz, F., 2010. Stone technology at the Middle Pleistocene site of Mata Menge, Flores, Indonesia. J Archaeol Sci 37, 451-473.

Clarkson, C., 2007. Lithics in the Land of the Lightening Brothers. The archaeology of Wardaman Country, Northern Territory. ANU E Press, Canberra.

Clarkson, C., Hiscock, P., 2011. Estimating original flake mass from 3D scans of platform area. J Archaeol Sci 38, 1062-1068.

Clarkson, C., Petraglia, M., Korisettar, R., Haslam, M., Boivin, N., Crowther, A., Ditchfield, P., Fuller, D., Miracle, P., Harris, C., 2009. The oldest and longest enduring microlithic sequence in India: 35 000 years of modern human occupation and change at the Jwalapuram Locality 9 rockshelter. Antiquity 83, 326-348.

Clarkson, C., Smith, M., Marwick, B., Fullagar, R., Wallis, L.A., Faulkner, P., Manne, T., Hayes, E., Roberts, R.G., Jacobs, Z., 2015. The archaeology, chronology and stratigraphy of Madjedbebe (Malakunanja II): A site in northern Australia with early occupation. J Hum Evol 83, 46-64.

Davidson, I., 2010. The colonization of Australia and its adjacent islands and the evolution of modern cognition. Curr Anthrop 51, S177-S189.

Davis, Z.J., Shea, J.J., 1998. Quantifying lithic curation: An experimental test of Dibble and Pelcin's original flake-tool mass predictor. J Archaeol Sci 25, 603-610.

Demeter, F., Shackelford, L., Westaway, K., Duringer, P., Bacon, A.-M., Ponche, J.-L., Wu, X., Sayavongkhamdy, T., Zhao, J.-X., Barnes, L., Boyon, M., Sichanthongtip, P., Sénégas, F., Karpoff, A.-M., Patole-Edoumba, E., Coppens, Y., Braga, J., 2015. Early modern Humans and morphological variation in Southeast Asia: Fossil evidence from Tam Pa Ling, Laos. PLoS ONE 10, e0121193.

Détroit, F., Corny, J., Dizon, E.Z., Mijares, A.S., 2013. “Small size” in the Philippine human fossil record: Is it meaningful for a better understanding of the evolutionary history of the negritos? Hum Biol 85, 45-66.

Détroit, F., Dizon, E., Falguères, C., Hameau, S., Ronquillo, W., Sémah, F., 2004. Upper Pleistocene Homo sapiens from the Tabon cave (Palawan, The Philippines): Description and dating of new discoveries. Comptes Rendus Palevol 3, 705-712.

Dibble, H., L., McPherron, S., P., 2006. The missing Mousterian. Curr Anthrop 47, 777.

Dibble, H.L., 1997. Platform variability and flake morphology: A comparison of experimental and archaeological data and implications for interpreting prehistoric lithic technological strategies. Lithic Technology, 150-170.

Environment and Development Division, 2003. Geology and Mineral Resources of Timor-Leste. United Nations, New York.

Eren, M.I., Lycett, S.J., Roos, C.I., Sampson, C.G., 2011. Toolstone constraints on knapping skill: Levallois reduction with two different raw materials. J Archaeol Sci 38, 2731-2739.

Eren, M.I., Roos, C.I., Story, B.A., von Cramon-Taubadel, N., Lycett, S.J., 2014. The role of raw material differences in stone tool shape variation: an experimental assessment. J Archaeol Sci 49, 472-487.

Foley, R., Lahr, M.M., 2003. On stony ground: Lithic technology, human evolution, and the emergence of culture. Evolutionary Anthropology: Issues, News, and Reviews 12, 109-122.

Glover, I., 1981. Leang Burung 2: An Upper Palaeolithic rock shelter in South Sulawesi, Indonesia. Modern Quaternary Research in South East Asia 6, 1-38.

Hayes, E.H., Fullagar, R.L.K., Clarkson, C., O'Connor, S., 2014. Usewear on the platform: 'use-flakes' and 'retouch-flakes' from northern Australia and Timor, in: Lemorini, C., Cesaro, S.N. (Eds.), An Integration of the Use-Wear and Residue Analysis for the Identification of the Function of Archaeological Stone Tools: Proceedings of the International Workshop. An Integration of the Use-Wear and Residue Analysis for the Identification of the Function of Archaeological Stone Tools: International Workshop, Rome, Italy. BAR International Series Volume 2649, pp. 77-90.

Hiscock, P., 2002. Quantifying the size of artefact assemblages. J Archaeol Sci 29, 251-258.

Kaifu, Y., Izuho, M., Goebel, T., 2015. Modern Human Dispersal and Behavior in Paleolithic Asia, in: Kaifu, Y., Izuho, M., Goebel, T., Sato, H., Ono, A. (Eds.), Emergence and diversity of modern human behavior in Paleolithic Asia. Texas A&M University Press, pp. 535-566.

Klein, R.G., 2009. The human career: Human biological and cultural origins. University of Chicago Press, Chicago.

Krushcke, J.K., 2011. Doing Bayesian Data Analysis: A Tutorial with R and BUGS. Academic Press, New York.

Langley, M.C., Clarkson, C., Ulm, S., 2011. From small holes to grand narratives: The impact of taphonomy and sample size on the modernity debate in Australia and New Guinea. J Hum Evol 61, 197-208.

Langley, M.C., O'Connor, S., 2015. 6500-Year-old Nassarius shell appliqués in Timor-Leste: Technological and use wear analyses. J Archaeol Sci 62, 175-192.

Langley, M.C., O'Connor, S., Piotto, E., 2016. 42,000-year-old worked and pigment-stained Nautilus shell from Jerimalai (Timor-Leste): Evidence for an early coastal adaptation in ISEA. J Hum Evol 97, 1-16.

Langley, M.C., O'Connor, S., 2016. An enduring shell artefact tradition from Timor-Leste: Oliva bead production from the Pleistocene to Late Holocene at Jerimalai, Lene Hara, and Matja Kuru 1 and 2. PloS one 11, e0161071.

Lewis, H., Paz, V., Lara, M., Barton, H., Piper, P., Ochoa, J., Vitales, T., Carlos, A.J., Higham, T., Neri, L., 2008. Terminal Pleistocene to mid-Holocene occupation and an early cremation burial at Ille Cave, Palawan, Philippines. Antiquity 82, 318-335.

Lohman, D.J., de Bruyn, M., Page, T., von Rintelen, K., Hall, R., Ng, P.K.L., Shih, H.-T., Carvalho, G.R., von Rintelen, T., 2011. Biogeography of the Indo-Australian Archipelago. Annual Review of Ecology, Evolution, and Systematics 42, 205-226.

Macgregor, O., 2005. Abrupt terminations and stone artefact reduction potential, in: Clarkson, C., Lamb, L. (Eds.), Rocking the Boat: Recent Australian Approaches to Lithic Reduction, Use and Classification. Archaeopress, Oxford.

Marwick, B., 2008. What attributes are important for the measurement of assemblage reduction intensity? Results from an experimental stone artefact assemblage with relevance to the Hoabinhian of mainland Southeast Asia. J Archaeol Sci 35, 1189-1200.
Marwick, B., 2016. Computational reproducibility in archaeological research: Basic principles and a case study of their implementation. J Archaeol Method Theory, 1-27.
Mellars, P., 2006. Going east: New genetic and archaeological perspectives on the modern human colonization of Eurasia. Science 313, 796.
Mijares, A.S., Détroit, F., Piper, P., Grün, R., Bellwood, P., Aubert, M., Champion, G., Cuevas, N., De Leon, A., Dizon, E., 2010. New evidence for a 67,000-year-old human presence at Callao Cave, Luzon, Philippines. J Hum Evol 59, 123-132.
Mijares, A.S.B., 2014. The Peñablanca flake tools: An unchanging technology? Hukay: Journal of the University of the Philippines Archaeological Studies Program 12, 13-34.
Moore, M., Brumm, A., 2009. Homo floresiensis and the African Oldowan, in: Hovers, E., Braun, D. (Eds.), Interdisciplinary Approaches to the Oldowan. Springer Netherlands, pp. 61-69.
Moore, M.W., Brumm, A., 2007. Stone artifacts and hominins in island Southeast Asia: New insights from Flores, eastern Indonesia. J Hum Evol 52, 85-102.
Moore, M.W., Sutikna, T., Jatmiko, Morwood, M.J., Brumm, A., 2009. Continuities in stone flaking technology at Liang Bua, Flores, Indonesia. J Hum Evol 57, 503-526.
Morwood, M.J., Brown, P., Jatmiko, Sutikna, T., et al., 2005. Further evidence for small-bodied hominins from the Late Pleistocene of Flores, Indonesia. Nature 437, 1012.
O'Connor, S., 2007. New evidence from East Timor contributes to our understanding of earliest modern human colonisation east of the Sunda Shelf. Antiquity 81, 523-535.
O'Connor, S., Robertson, G., Aplin, K., 2014a. Are osseous artefacts a window to perishable material culture? Implications of an unusually complex bone tool from the Late Pleistocene of East Timor. J Hum Evol 67, 108-119.
O'Connor, S., Robertson, G., Aplin, K.P., 2014b. Are osseous artefacts a window to perishable material culture? Implications of an unusually complex bone tool from the Late Pleistocene of East Timor. J Hum Evol 67, 108-119.
O'Connor, S., Ono, R., Clarkson, C., 2011. Pelagic fishing at 42,000 years before the present and the maritime skills of modern humans. Science 334, 1117-1121.
Parnell, A., 2016. Bchron: Radiocarbon Dating, Age-Depth Modelling, Relative Sea Level Rate Estimation, and Non-Parametric Phase Modelling. R package version 4.2.5. https://CRAN.R-project.org/package=Bchron.
Parnell, A.C., Buck, C.E., Doan, T.K., 2011. A review of statistical chronology models for high-resolution, proxy-based Holocene palaeoenvironmental reconstruction. Quaternary Science Reviews 30, 2948-2960.
Patole-Edoumba, E., 2009. A typo-technological definition of Tabonian industries. Bulletin of the Indo-Pacific Prehistory Association 29, 21-25.
Patole-Edoumba, E., Pawlik, A.F., Mijares, A.S., 2012. Evolution of prehistoric lithic industries of the Philippines during the Pleistocene. Comptes Rendus Palevol 11, 213-230.

881 Pawlik, A.F., 2012. Behavioural complexity and modern traits in the Philippine Upper
882 Palaeolithic. Asian Persp 51, 22-46.
883 Petraglia, M., Clarkson, C., Boivin, N., Haslam, M., Korisettar, R., Chaubey, G.,
884 Ditchfield, P., Fuller, D., James, H., Jones, S., Kivisild, T., Koshy, J., Lahr,
885 M.M., Metspalu, M., Roberts, R., Arnold, L., 2009. Population increase and
886 environmental deterioration correspond with microlithic innovations in South
887 Asia ca. 35,000 years ago. Proceedings of the National Academy of Sciences
888 106, 12261-12266.
889 R Core Team, 2015. R: A language and environment for statistical computing. R
890 Foundation for Statistical Computing. http://www.R-project.org/. Vienna,
891 Austria.
892 Rabett, R.J., 2011. Techno-modes, techno-facies and palaeo-cultures: Change and
893 continuity in the Pleistocene of Southeast, Central and North Asia,
894 Investigating Archaeological Cultures. Springer, pp. 97-135.
895 Reepmeyer, C., O'Connor, S.U.E., Brockwell, S., 2011. Long-term obsidian use at the
896 Jerimalai rock shelter in East Timor. Archaeol Oceania 46, 85-90.
897 Reimer, P.J., Bard, E., Bayliss, A., Beck, J.W., Blackwell, P.G., Ramsey, C.B., Buck,
898 C.E., Cheng, H., Edwards, R.L., Friedrich, M., 2013. IntCal13 and Marine13
899 radiocarbon age calibration curves 0–50,000 years cal BP. Radiocarbon 55,
900 1869-1887.
901 Reti, J.S., 2016. Quantifying Oldowan stone tool production at Olduvai Gorge,
902 Tanzania. PLoS ONE 11, e0147352.
903 Reynolds, T.E.G., 1993. Problems in the Stone Age of South-East Asia. Proc Prehist
904 Soc 59, 1-15.
905 Sahle, Y., Morgan, L.E., Braun, D.R., Atnafu, B., Hutchings, W.K., 2014.
906 Chronological and behavioral contexts of the earliest Middle Stone Age in the
907 Gademotta formation, main Ethiopian rift. Quaternary International 331, 6-19.
908 Shipton, C., Clarkson, C., Pal, J., Jones, S., Roberts, R., Harris, C., Gupta, M.,
909 Ditchfield, P., Petraglia, M., 2013. Generativity, hierarchical action and
910 recursion in the technology of the Acheulean to Middle Palaeolithic transition:
911 A perspective from Patpara, the Son Valley, India. J Hum Evol 65, 93-108.
912 Sutikna, T., Tocheri, M.W., Morwood, M.J., Saptomo, E.W., Jatmiko, Awe, R.D.,
913 Wasisto, S., Westaway, K.E., Aubert, M., Li, B., Zhao, J.-x., Storey, M.,
914 Alloway, B.V., Morley, M.W., Meijer, H.J.M., van den Bergh, G.D., Grün, R.,
915 Dosseto, A., Brumm, A., Jungers, W.L., Roberts, R.G., 2016. Revised
916 stratigraphy and chronology for Homo floresiensis at Liang Bua in Indonesia.
917 Nature advance online publication.
918
919
920

921

922 **Table 1. Radiocarbon dates for Jerimalai square A and B. Dates calibrated using the**

923 **IntCal13 curve (Reimer et al., 2013) by Bchron 4.1.2 (Parnell, 2016).**

924

925

926

Square	Spit	Depth below surface (m)	Material	Radiocarbon Age (years)	Radiocarbon Error (years)	Calibrated 2.5% credible interval (years)	Calibrated 97.5% credible interval (years)	Lab code
A	3	0.06	charcoal	2570	34	2515	2751	Wk-19224
A	5	0.092	charcoal	3245	39	3390	3562	Wk-19225
A	6	0.115	*Turbo*	5341	41	6003	6261	Wk-18154
A	12	0.306	*Turbo*	5567	44	6294	6436	Wk-18155
A	13	0.339	*Turbo*	5549	62	6232	6453	Wk-17829
A	21	0.525	*Turbo*	5909	40	6661	6832	Wk-19226

A	26	0.639	*Haliotis* cf. *varia Turbo*	10110	79	11363	11997	Wk-18156
A	27	0.662	*Turbo*	19952	235	23486	24594	Wk-17830
A	38	0.877	*Turbo*	13658	91	16245	16785	Wk-19227
A	46	1.119	*Trochus*	38255	596	41565	43172	Wk-17831
B	3	0.067	charcoal	124	32	15	268	Wk-19228
B	4	0.093	*Turbo*	4962	50	5608	5869	Wk-19229
B	9	0.203	*Trochus*	4580	42	5072	5442	Wk-19230
B	16	0.381	*Trochus*	4867	42	5491	5700	Wk-18157
B	21	0.502	*Trochus*	5595	43	6305	6463	Wk-18158
B	23	0.543	*Trochus*	5694	45	6392	6615	Wk-18159

B	33	0.776	*Trochus*	5939	45	6672	6877	Wk-17832
B	34	0.898	Shell bead/*Nautilus*	6118	41	6890	7149	Wk-19316
B	40	0.912	*Trochus*	8879	78	9678	10188	Wk-19231
B	41	0.952	*Oliva* shell bead	6223	26	7024	7241	Wk-30500
B	42	0.967	*Oliva* shell bead	5575	27	6307	6402	Wk-30501
B	43	0.993	*Oliva* shell bead	13901	45	16693	16992	Wk-30502
B	46	1.054	*Oliva* shell bead	9457	32	10597	10760	Wk-30503
B	49	1.135	*Haliotis* cf. *varia*	14007	146	16545	17426	Wk-18160
B	50	1.152	*Haliotis* cf. *varia*	13778	43	16521	16810	Wk-30504
B	56	1.305	*Turbo*	35387	534	38832	41074	Wk-19232

	B	66	1.624	*Trochus*	37267	453	40993	42275	Wk-1783 3

927

928

929 **Table 2. Definitions of artefact classes.**

930

Class	Definition
Distal	Retouch concentrated on the distal end of a flake
Lateral	Retouch on the lateral margin
Notched	Deep concave retouch forming a distinct notch
Lateral and Distal	Side and end retouch
Double Side and End	Retouch located on both lateral margins as well as the distal margin
Denticulated	A retouched flake with a series of (more than two) adjacent notches forming a 'toothed' edge
Notched Lateral and Distal	Retouch on the side and distal margins
Drill Like Retouch\Edge Damage	A retouched and crushed projection resembling a drill tip
Platform Faceting	Faceting of the platform edge to create a steep and robust platform
Flake with Old Ventral on Dorsal	Flake with remnant ventral portion on the dorsal surface indicating it was struck from a flake core
Truncated Flake	A flake broken in two by percussion
Flake With Gloss	A flake with a highly reflective polish on the lateral margin most likely formed from intensive use on silica rich plants
Striated Haematite	Haematite with multiple overlapping scratches indicative of dry grinding

Microblade	A small (<4cm long) elongate flake with parallel or tapering margins with one or more longitudinal ridges
Levallois-like Flake	Flake with radial dorsal flake scar pattern and faceted platform
Burin Spall	Long narrow flake
Pointed Flake with Facetted Platform	Flake with converging margins with a faceted platform
Bipolar Flake	Flake produced from a bipolar core with crushed initiations on opposed ends and a typically flat and sheared ventral surface.
Éclat Débordant	A flake struck from the edge of a bifacial core preserving alternating imitations on its dorsal ridge.
Cortical Flake	Flake with cortex covering the entire dorsal surface
Redirecting Flake	A flake with remnant platform edges on the dorsal surface signifying a reorientation of flaking orientation and the creation of a new platform
Chopper	Typically elongate nodule with unifacial or bifacial flaking at one end resembling a strong cutting blade. This implement can also typically be classified as a single platform or bifacial core.
Anvil	Natural stone showing pitting and abrasion on an otherwise unaltered surface as a result of percussive actions such as bipolar flaking
Semi Discoidal	Core with two distinct hemispheres showing bifacial radial flaking around part of the core perimeter
Faceted Radial	Core with two hemispheres with radial flaking on one or both hemispheres with a faceted platform. These cores resemble unstruck Levallois core.

Levallois	A core with two hierarchically organised hemispheres with an upper flake removal surface and a lower platform creation and maintenance surface. Levallois cores typically show signs of platform preparation in the form of faceting of the lower surface adjacent to large removals on the upper surface that exploit areas of high mass created by the formation of lateral and distal convexities. The convexities themselves are often removed in the act of striking a Levallois flake.
Truncated Faceted Flake	A flake struck from the ventral surface of a large flake. The flake is initiated from a steep faceted edge (truncation). The flakes removed from the original ventral surface are typically large relative to the ventral area. Truncated faceted flakes take advantage of natural lateral and distal convexities present in the undulating ventral surface of the large flake. Kombewa flakes and flakes with varying amounts of remnant ventral surface on the newly created dorsal surface are among the products of flaking truncated faceted cores.
Bipolar	Removal of flakes by resting a nucleus on an anvil and imparting force through a crushing blow with a hammerstone
Bidirectional	Flakes initiated on a single face from opposed core edges
Single Platform	Flakes initiated only from a single platform edge on a core
Multiplatform	Flakes initiated from several platforms at varying orientations on a core

931

932

933

Table 3. Frequencies of dominant raw materials by depositional phase.

	phase 1	phase 2	phase 3	phase 4
Chert	677	1088	1789	818
Obsidian	0	5	1	5
Quartz	0	1	9	7
Quartzite	2	2	15	11
Silcrete	9	11	13	13
Unknown	7	7	2	2
Volcanic	33	30	73	89

Table 4. Highest density intervals (95%) for the posterior distributions of the interactions between phases and raw material frequencies.

	HDI low	HDI high
phase 1.v.phase 2	-0.818	0.075
phase 2.v.phase 3	-0.860	-0.106
phase 3.v.phase 4	-0.273	0.421

Table 5. Table of frequencies of each class of breakage by phase.

	phase 1	phase 2	phase 3	phase 4

long	85	66	125	61
trans	192	256	437	136
flake	676	1081	1769	810

945

946

947 **Table 6. Highest density intervals (95%) for the posterior distributions of the interactions**
948 **between phases and flake breakage classes. There are credible differences between all**
949 **phases.**

950

	HDI low	HDI high
phase 1.v.phase 2	-0.324	-0.071
phase 2.v.phase 3	-0.661	-0.439
phase 3.v.phase 4	0.767	1.003

951

952

953

954 **Table 7. Highest density intervals (95%) for the posterior distributions of the interactions**
955 **between phases and heat treatment. There are credible differences in phases 1 to 2, and**
956 **phases 2 to 3.**

957

	HDI low	HDI high
phase 1.v.phase 2	-0.627	-0.373
phase 2.v.phase 3	-0.491	-0.284
phase 3.v.phase 4	0.685	0.942

958

959

960 **Table 8. Summary of attributes of chert complete flakes from Jerimalai. Each cell contains**
961 **median ± interquartile range unless otherwise indicated.**

962

Depositional phase (# chert flakes)	phase 1 (728)	phase 2 (1144)	phase 3 (1907)	phase 4 (946)
Length (mm)	8.44±6.97	8.71±6.97	9.04±6.16	10.55±8.56
Width (mm)	7.92±5.87	8.33±6.32	8.45±6.20	9.62±7.54
Thickness (mm)	1.97±2.30	1.95±2.15	2.05±2.03	2.54±2.85
Mass (g)	0.16±0.46	0.16±0.50	0.17±0.44	0.31±0.85
Plat. width (mm)	5.77±4.91	5.58±4.62	5.95±5.23	7.24±5.68
Plat. thickness (mm)	1.94±2.08	1.76±1.77	1.95±1.81	2.54±2.71
Dorsal scars	4.00±2.00	4.00±3.00	4.00±2.00	4.00±2.00
Dorsal cortex %	0.00±0.00	0.00±0.00	0.00±0.00	0.00±0.00

Overhang removal *n* (%)	407.00±55.91	633.00±55.33	1136.00±59.57	553.00±58.46

963

964

965 **Table 9. Highest density intervals (95%) for the posterior distributions of the interactions**

966 **between phases and flake mass.**

967

	HDI low	HDI high
1.v.2	-0.108	0.194
2.v.3	-0.200	0.037
3.v.4	-0.553	-0.293

968

969

970

Table 10. Summary of metric attributes of chert complete cores from Jerimalai. Each cell contains median ± interquartile range unless otherwise indicated.

Depositional phase (# cores)	phase 1 (50)	phase 2 (37)	phase 3 (56)	phase 4 (46)
Length (mm)	3.05±6.51	2.12±3.57	2.17±3.03	3.29±5.80
Width (mm)	22.63±13.43	18.72±7.61	17.36±7.91	18.38±12.66
Thickness (mm)	14.80±9.48	14.78±7.53	13.44±6.24	14.26±8.51
Mass (g)	9.70±7.20	7.33±5.61	8.52±4.50	9.54±4.09
Flake scars	11.00±6.00	11.00±6.00	11.00±6.00	11.00±6.00
Cortex %	0.00±10.00	0.00±10.00	0.00±10.00	0.00±10.00
Rotations	3.00±1.00	3.00±1.00	3.00±1.00	3.00±1.00

Table 11. Highest density intervals (95%) for the posterior distributions of the interactions between phases and core mass, both squares.

	HDI low	HDI high
1.v.2	1.034	20.519
2.v.3	-8.236	8.658
3.v.4	-9.676	6.440

Table 12. Highest density intervals (95%) for the posterior distributions of the interactions between phases and flake and core cortex.

	cores		flakes	
	HDI low	HDI high	HDI low	HDI high
1.v.2	-1.902	6.755	-0.413	1.714
2.v.3	-8.598	0.690	-1.111	0.588
3.v.4	-0.802	7.872	-2.348	-0.368

Table 13. Highest density intervals (95%) for the posterior distributions of the interactions between phases and retouch frequency and length.

	Retouch frequency		Retouch length	
	HDI low	HDI high	HDI low	HDI high
1.v.2	-1.802	7.074	-2.848	6.633
2.v.3	-8.733	0.748	-8.410	2.168
3.v.4	-0.859	7.908	-4.107	6.174

994

995

996 **Table 14. Summary of retouch indices for retouched pieces recovered from Jerimalai.**
997 **GIUR = Geometric Index of Unifacial Retouch, II = Index of Invasiveness, % = percent of**
998 **perimeter with retouch.**

999

1000

Square	Spit	Phase	Type	GIUR	II	%
B	4	4	Double Side and End (steep edged)	0.83	0.28	50.00
B	4	4	Double Side	0.85	0.34	33.04
B	5	4	Side Ventral	NA	0.06	11.94
B	10	4	Side	0.37	0.09	18.66
B	10	4	End	0.46	0.03	11.80
B	12	4	Drill?	0.55	0.19	43.10
B	14	4	Notch	0.62	0.09	20.00
B	19	4	Denticulate	0.19	0.16	27.68
B	22	3	Notch (Ventral)	NA	0.09	40.69
B	25	3	Bifacial End	0.37	0.09	17.36
B	34	3	Side and End (Alternating bifacial)	0.38	0.12	28.23
B	38	3	Notch (Ventral)	NA	0.06	14.59
B	39	3	Concave Bifacial side and end	0.80	0.56	60.15
B	40	2	Side	0.26	0.09	21.31

	A	43	1	Bec			0.52	0.16	29.51

1001

1002

1003

1004

1005

1006 **Table 15. Summary of proportions and classes. 'Proportions' refers to the proportion of spits in**

1007 **each depositional phase containing a given class.**

1008

	Phase	1	2	3	4
	Type	%	%	%	%
Retouch	Distal	23.81	12.50	10.26	40.00
	Lateral	19.05	18.75	10.26	32.00
	Notched	14.29	0.00	7.69	24.00
	Lateral and Distal	9.52	6.25	0.00	4.00
	Double Side and End	9.52	12.50	2.56	20.00
	Denticulated	0.00	3.13	2.56	4.00
	Notched Lateral and/or Distal	0.00	6.25	5.13	0.00
	Retouched Pointed Projections (Piercer/Drill-like)	4.76	0.00	0.00	8.00
	Old Ventral Surface on Dorsal\Faceted Platform	52.38	9.38	30.77	32.00
Flake Features	Platform Faceting	71.43	34.38	74.36	76.00
	Flake With Old Ventral on Dorsal	19.05	12.50	23.08	32.00
	Truncated Flake	4.76	9.38	2.56	0.00
	Flake With Gloss	0.00	0.00	2.56	4.00
Ground	Striated Haematite	0.00	0.00	5.13	4.00
Technological	Microblade	23.81	6.25	20.51	8.00
Types	Levallois-like Flake	9.52	0.00	5.13	0.00
	Burin Spall	14.29	12.50	2.56	16.00
	Pointed Flake with Facetted Platform	14.29	0.00	0.00	0.00
	Bipolar Flake	9.52	21.88	7.69	16.00

	Éclat Débordant	0.00	9.38	5.13	0.00
	Cortical Flake	4.76	0.00	2.56	12.00
	Redirecting Flake	33.33	21.88	17.95	44.00
	Chopper Anvil	0.00	3.13	0.00	4.00
Cores	Discoidal/Semi Discoidal	4.76	6.25	0.00	8.00
	Faceted Radial Levallois-like	14.29	3.13	2.56	12.00
	Truncated Faceted	14.29	3.13	0.00	4.00
	Bipolar	9.52	9.38	7.69	16.00
	Bidirectional	4.76	3.13	2.56	8.00
	Single Platform	9.52	0.00	2.56	16.00
	Multiplatform	23.81	12.50	10.26	16.00

1012

1013

1014

1015

1016

Figure 1. Map showing key locations mentioned in the text.

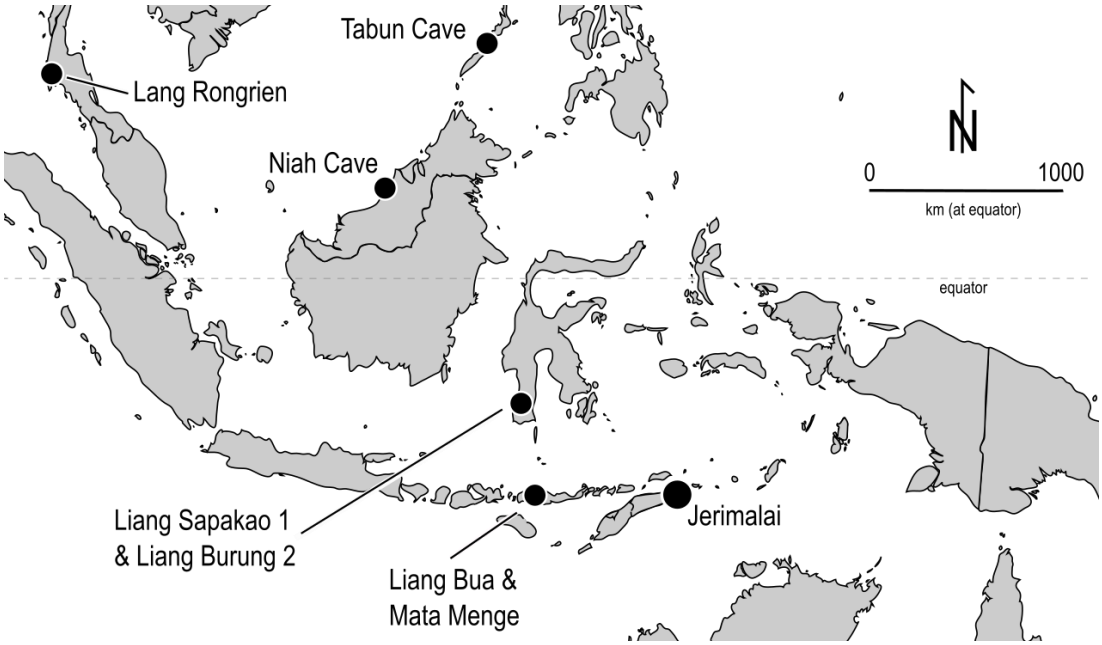

Figure 2. Depth-age distribution for radiocarbon dates from Jerimalai.

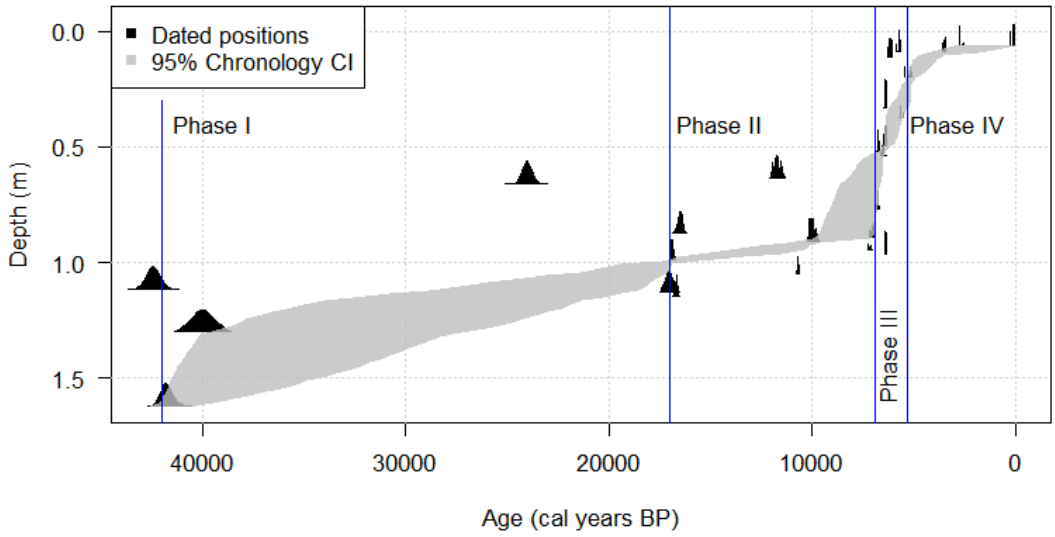

Figure 3. Discard rates of chert artefacts over time at Jerimalai. Each point is an excavation unit (spit). The lines are locally weighted regression lines (span = 0.4) to aid in visualising the trend of increased discard in the upper part of the deposit.

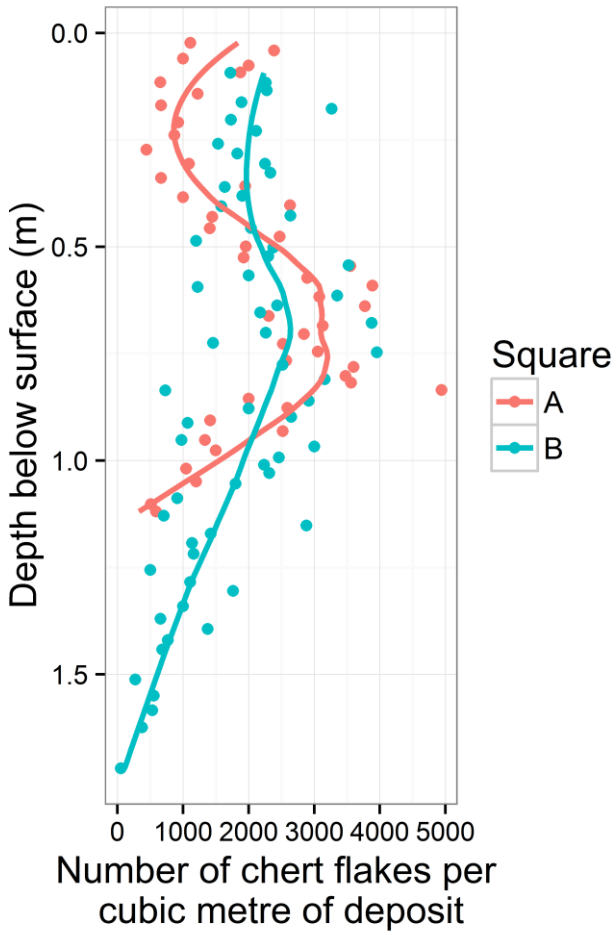
0.0
0.5
1.0
1.5
Depth below surface (m)
0
1000
2000
3000
4000
5000
Number of chert flakes per cubic metre of deposit
Square
A
B

1033

1034

Figure 4. Flakes with edge-gloss (1,2), striated haematite (square B spit 11, square B spit 23) and a piece of obsidian (square B spit 5) from Jerimalai (scale bar for each artefact = 10 mm).

Figure 5. Distribution of core and complete flake mass by depositional phases.

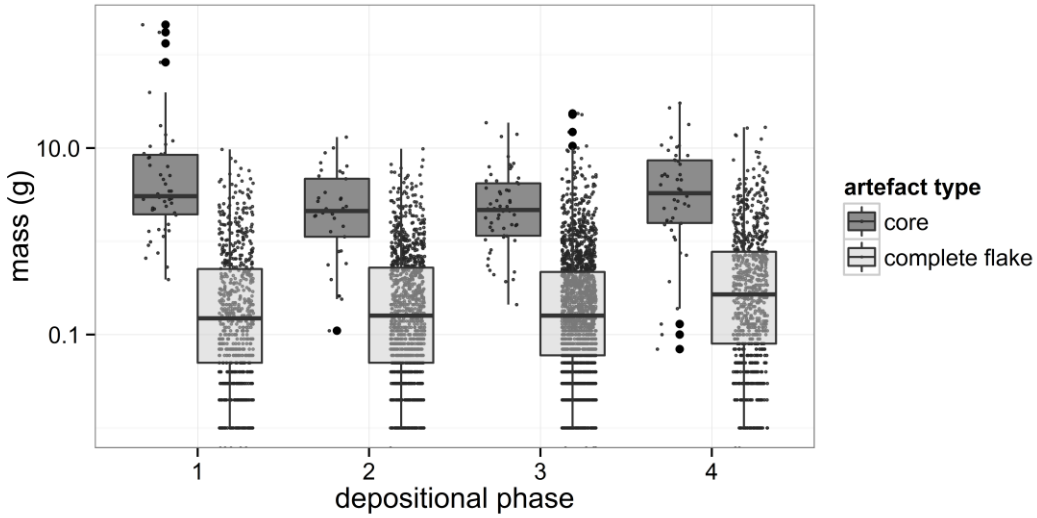

Figure 6. Frequency of flake platform category for chert complete flakes at Jerimalai square B. subplot: distribution of platform area by category.

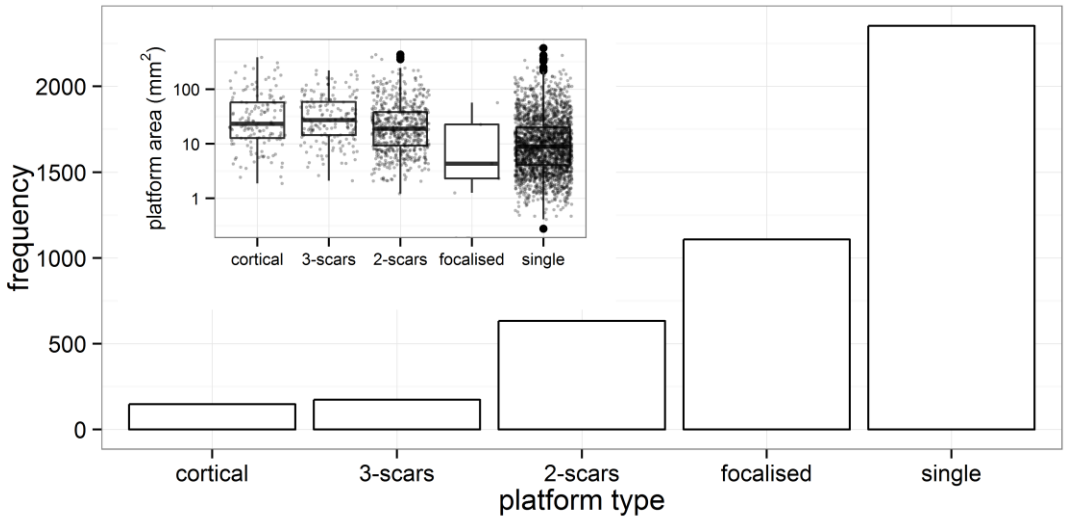

Figure 7. Distributions of core and flake cortex by depositional phase at Jerimalai square B.

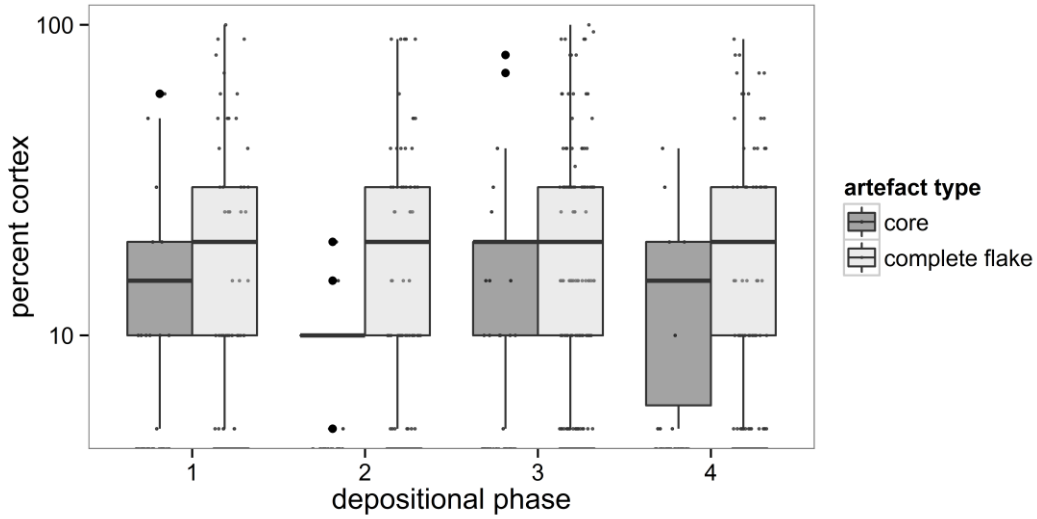

Figure 8. Cores recovered from Jerimalai. Differences in core mass by type.

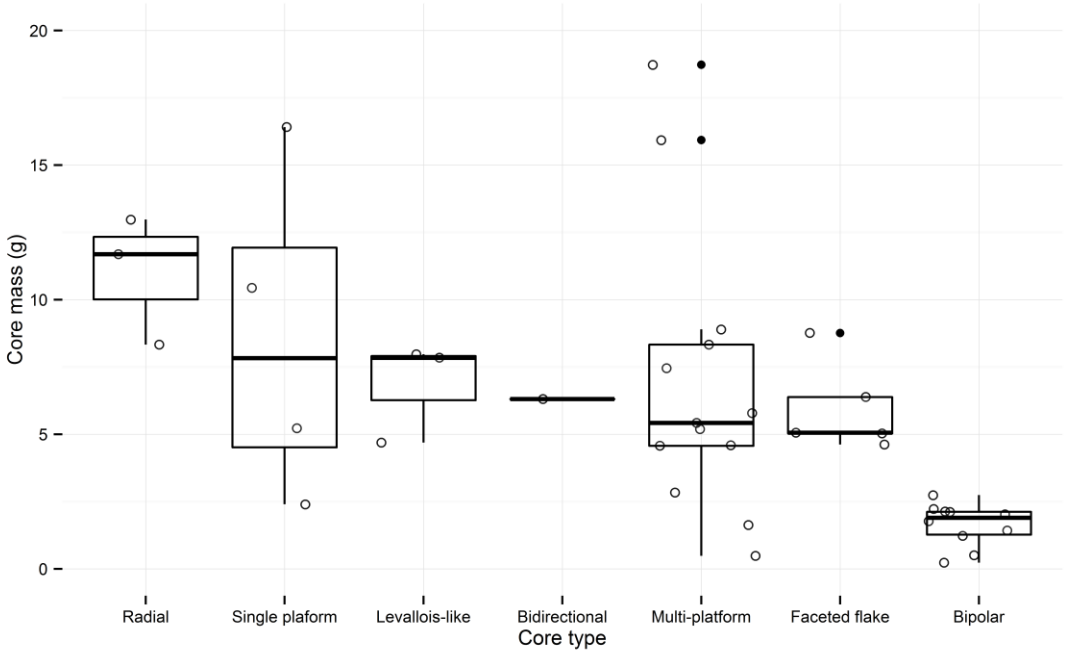

Figure 9. Example of a flake (square B spit 64) that has been steeply faceted around the margins to remove invasive flakes from the ventral surface (left = ventral, right = dorsal, top = faceted platform). Scale bar represents 1cm.

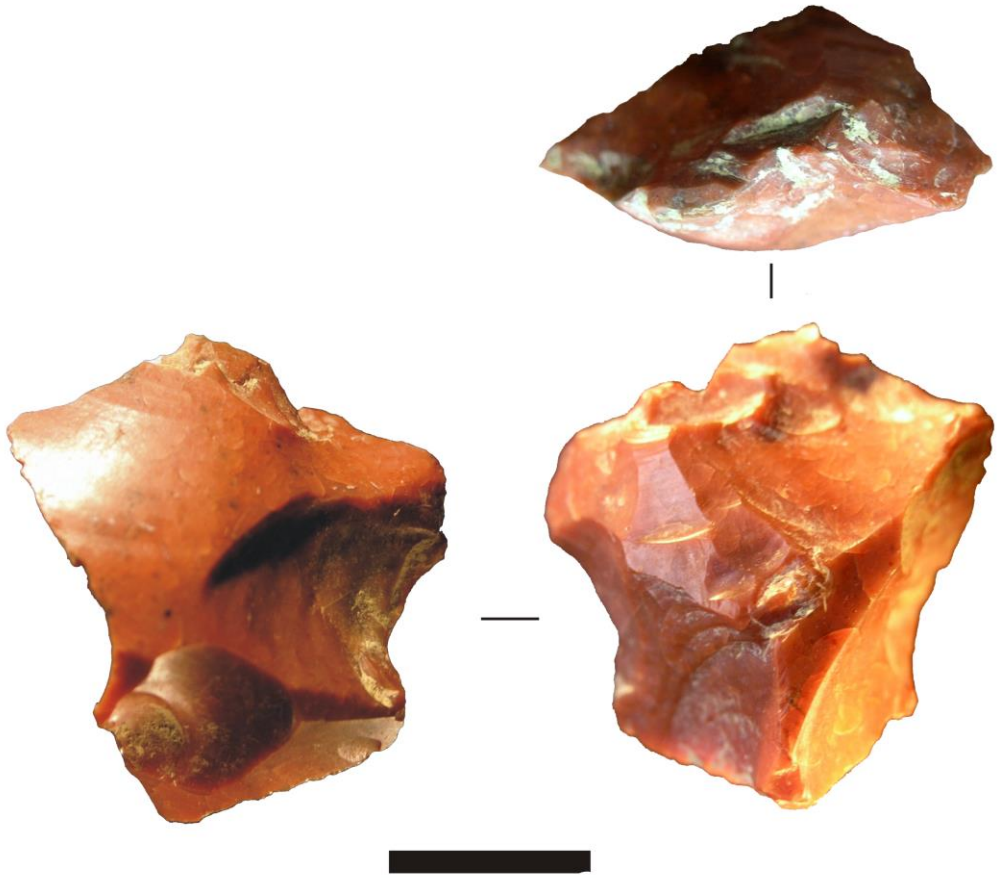

Figure 10. One possible hypothetical reduction scheme for the Jerimalai assemblage, showing flake products resulting from various stages of flake production from the ventral surfaces of larger flakes.

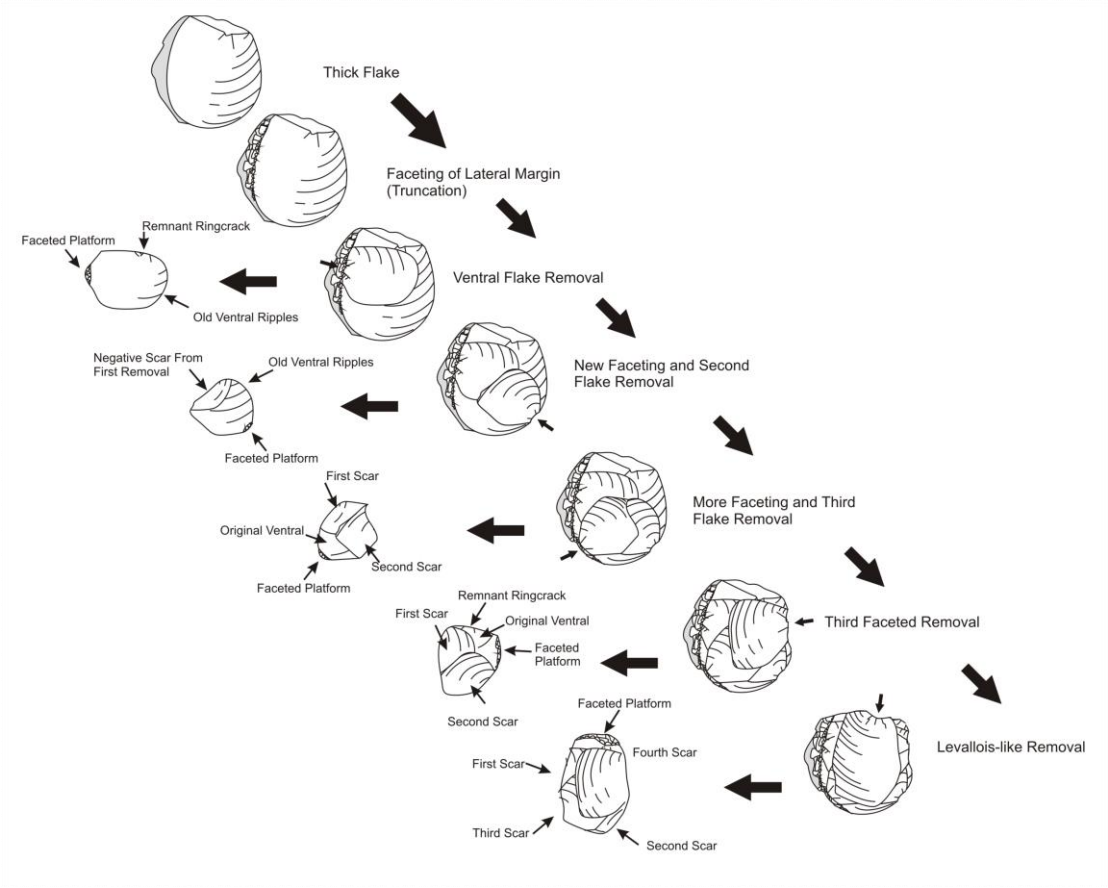

Figure 11. Examples of flakes struck from the ventral surfaces of large flakes showing faceted or unfaceted platforms. 1: square B spit 60, faceted, 2: square B spit 19, unfaceted, 3: square B spit 66, unfaceted, 4: square B spit 23, faceted, 5: square B spit 58, faceted, 6: square B spit 63, Kombewa flake, 7: square B spit 60, unfaceted, 8: square B spit 63, unfaceted, 9: square B spit 63, faceted, 10: square B spit 24, faceted, 11: square B spit 22, unfaceted, 12: square B spit 29, Kombewa flake with faceted platform. Scale bar represents 1cm.

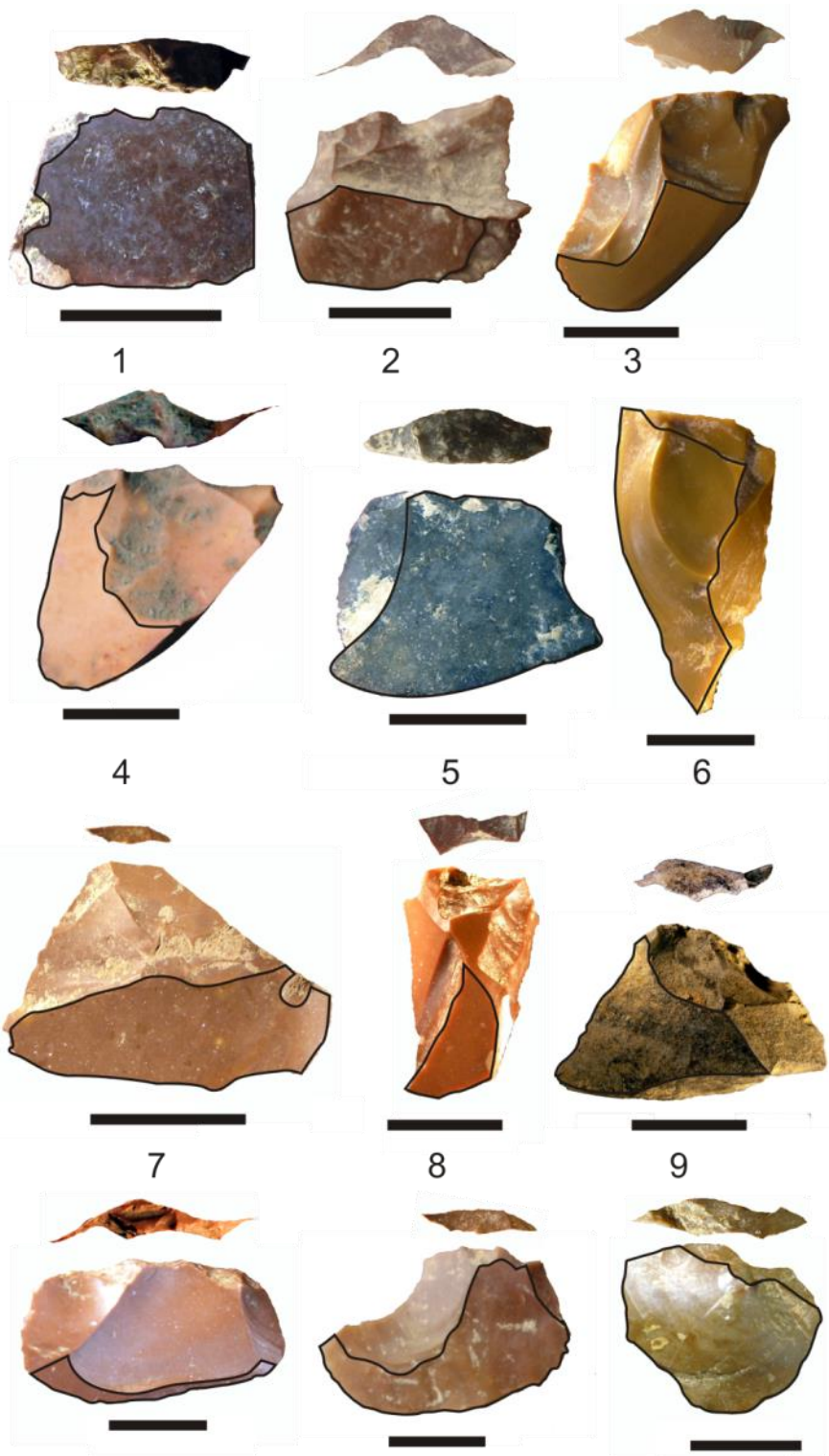
1
2
3
4
5
6
7
8
9
10
11
12

Figure 12. Flakes resembling Levallois flakes with faceted platforms and radial dorsal scar patterns. 1: square A spit 24, 2: square A spit 32, 3: square A spit 29, 4: square A spit 18, 5: square B spit 66, note small area of remaining ventral surface on the top left portion of the flake, 6: square A spit 44. Scale bar represents 1cm.

1124

Figure 13. Small Levallois-like cores with hierarchically organised surfaces and faceted platforms. 1: square B spit 37, broken half of overshot Levallois-like core, 2: square B spit 54, 3: square B spit 63, 4: square B spit 52, 5: square A spit 33, 6: square B spit 52. Scale bar represents 1cm.

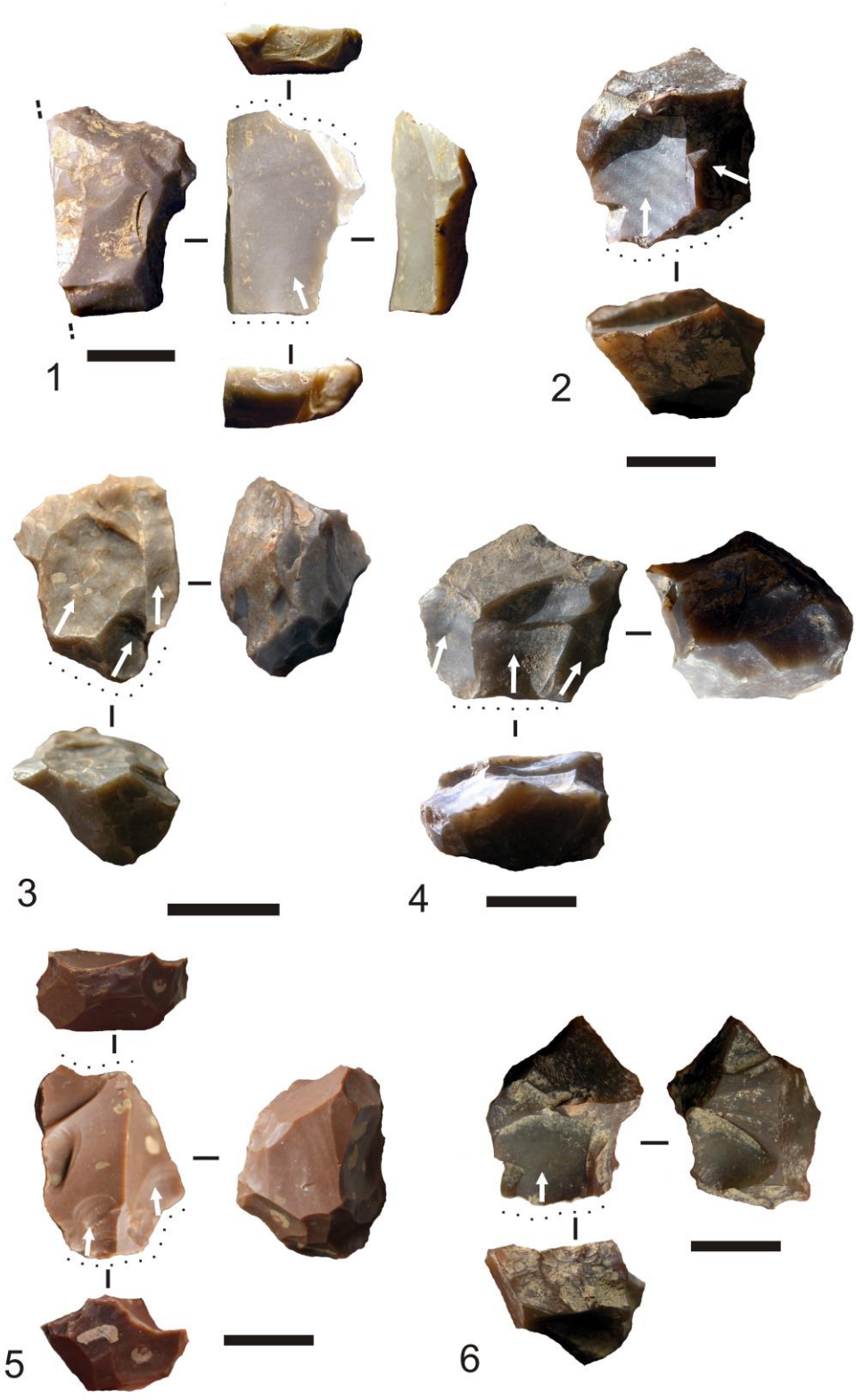

1132

1133

1134

Figure 14. Locations of retouch on chert flakes by depositional unit at Jerimalai.

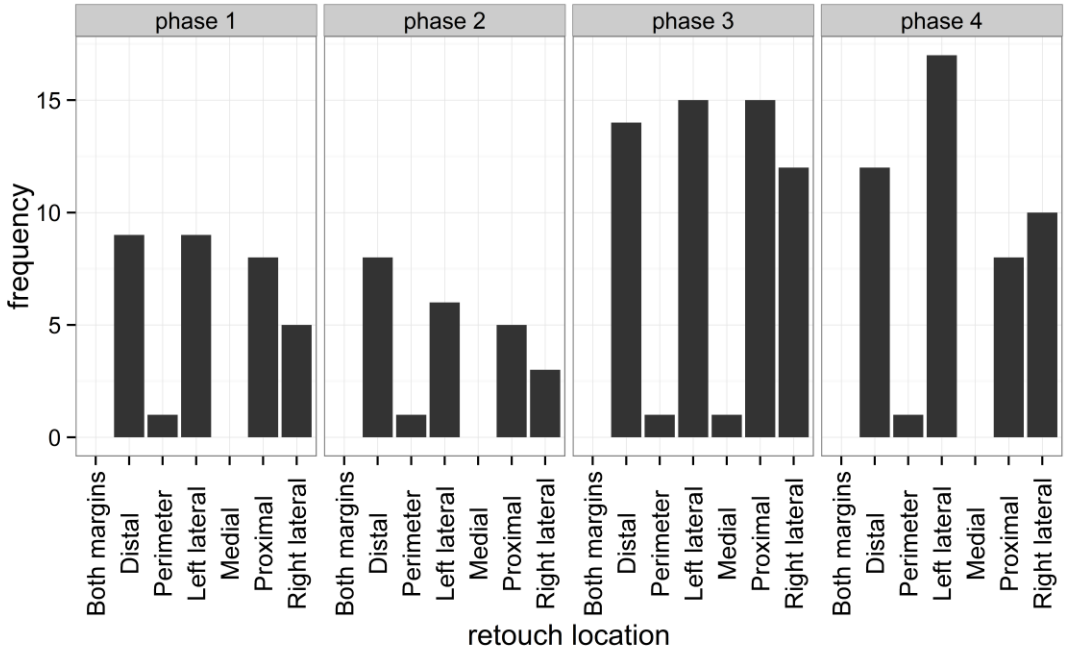

Figure 15. Distribution of flake masses for retouched and unretouched flakes by depositional unit at Jerimalai square B.

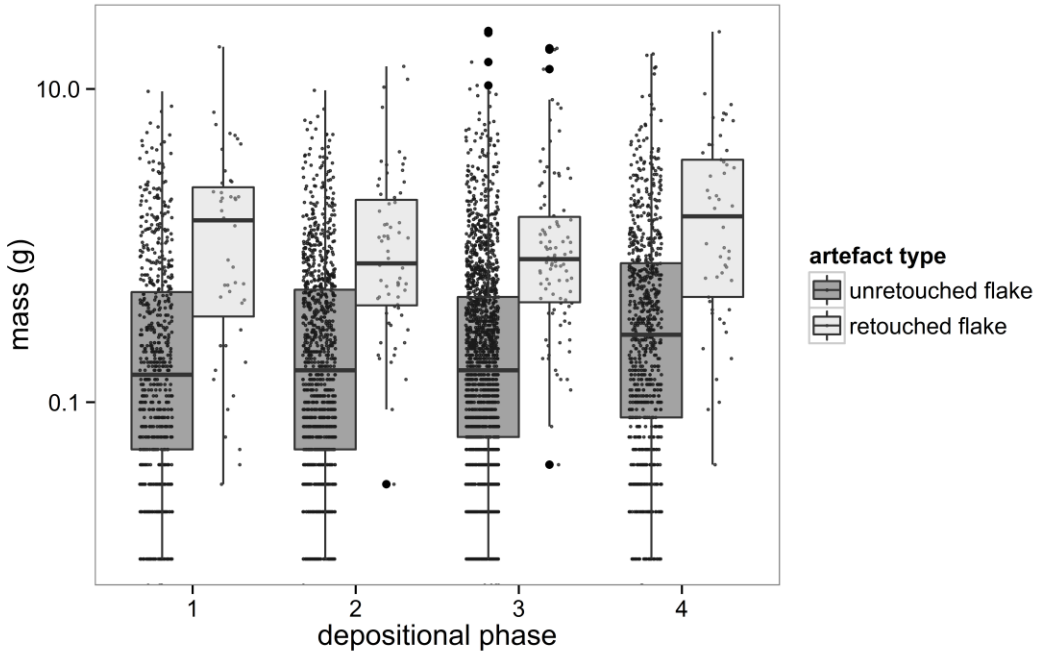

1143

1144

1145

Figure 16. Retouched flakes recovered from Jerimalai. 1: end notch, 2: square A spit 34, notch, 53 square A spit 37, denticulate, 4: square A spit 23, denticulate, 5: steep double side and end, 6: notched side and end, 7: notched double side and end, 8: bifacial tip?, 9: square B spit 63, end notch, 10: square B spit 37, bifacial tip, 11: square B spit 28, notch with bifacial retouch. Scale bar represents 1cm.

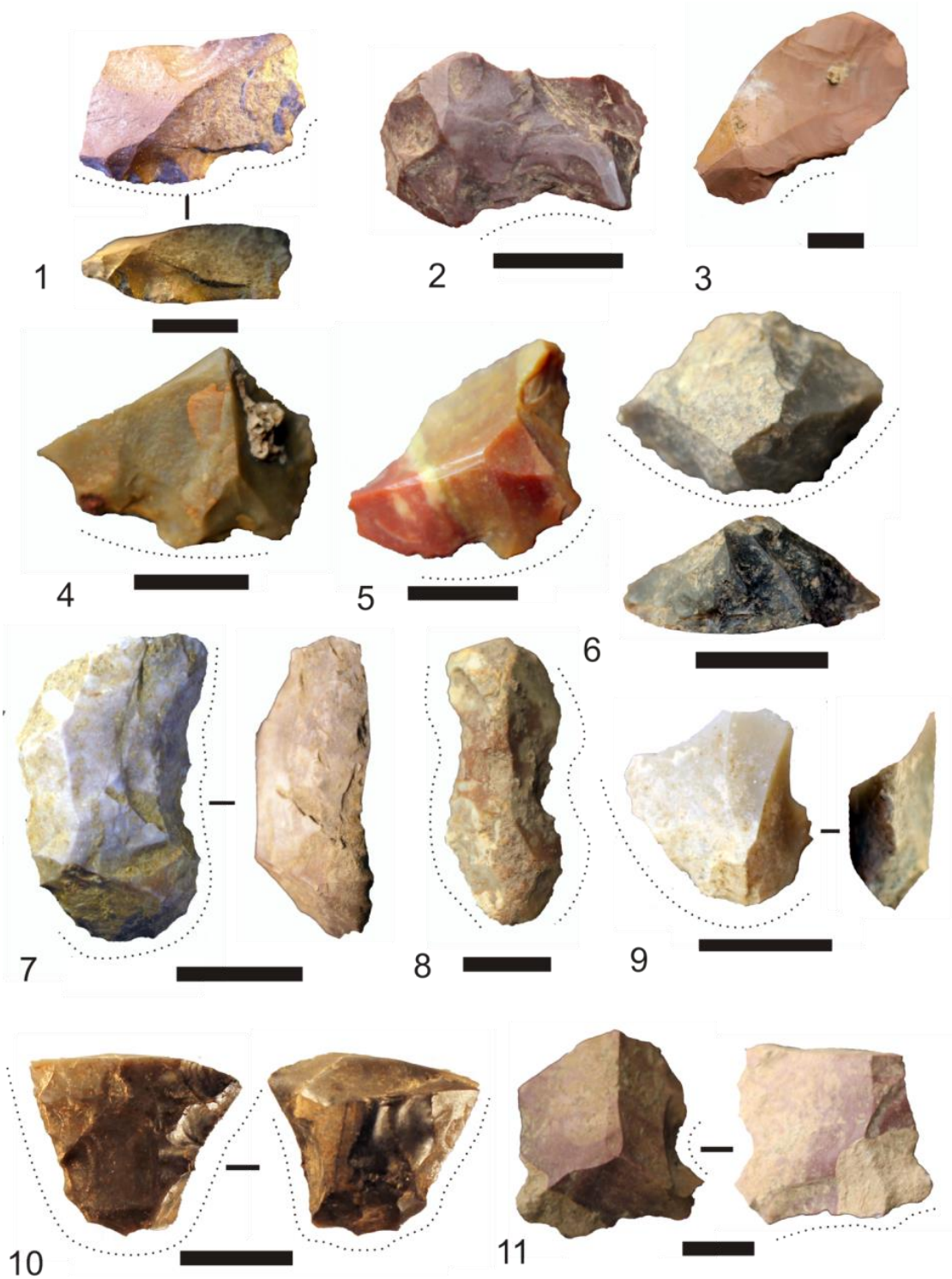
1
2
3
4
5
6
7
8
9
10
11

Figure 17. Pieces with retouched projections. 1: square A spit 31, 2: square A spit 42, 3: square A spit 21, 4: square B spit 4, 5: square B spit 12, showing possible use-damaged projection (lower image). Scale bar represents 1cm.

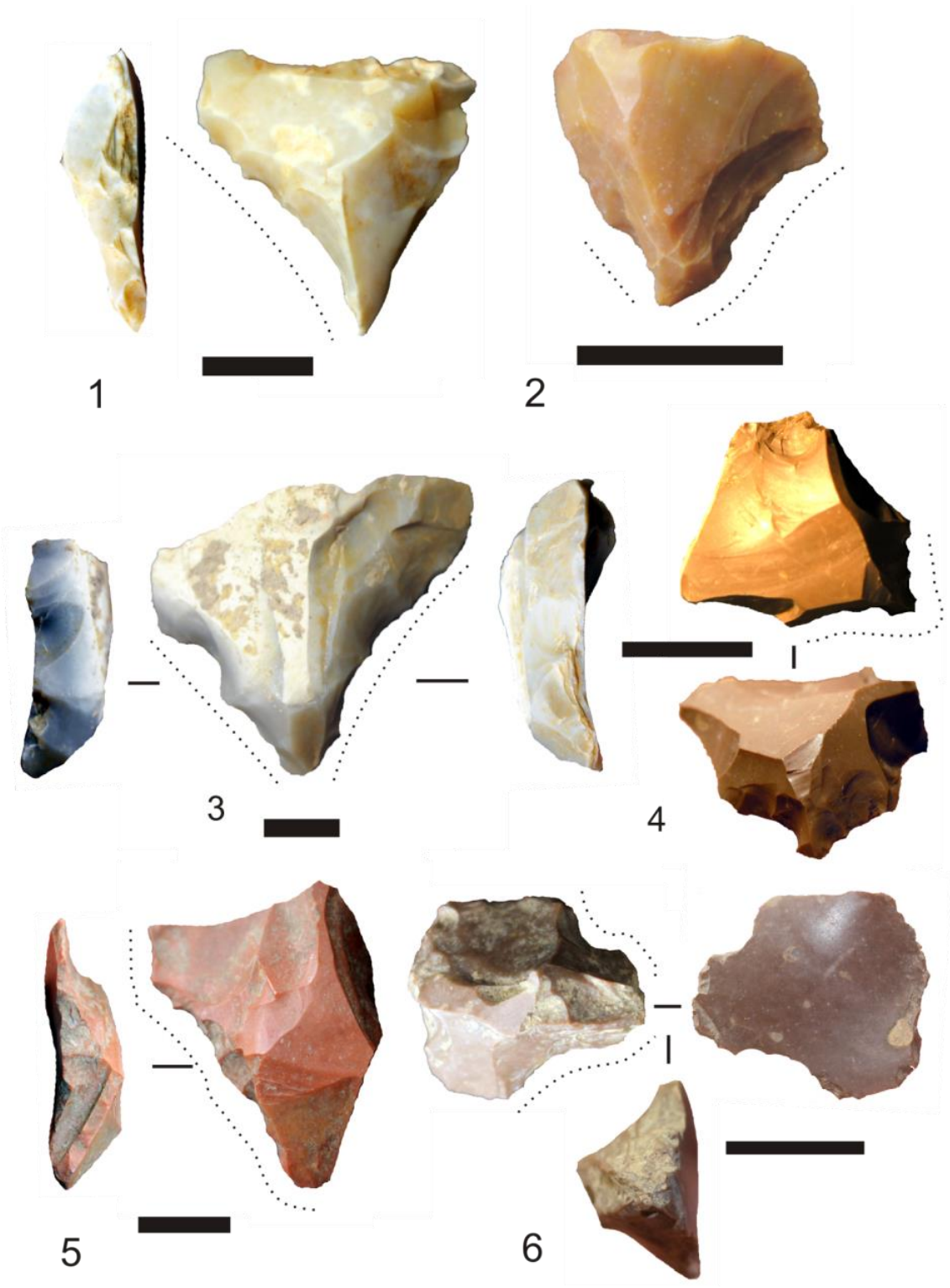
1
2
3
4
5
6

1169

1170